INTERNATIONAL MONETARY FUND

A Multi-Country Study of Forward-Looking Economic Losses from Floods and Tropical Cyclones

Michele Fornino, Mahmut Kutlukaya, Caterina Lepore and Javier Uruñuela López

WP/24/141

2024
JUL

WORKING PAPER

 WP/24/141

IMF Working Paper

Statistics Department and Monetary and Capital Market Department

A Multi-Country Study of Forward-Looking Economic Losses from Floods and Tropical Cyclones

Prepared by Michele Fornino, Mahmut Kutlukaya, Caterina Lepore and Javier Uruñuela López

Authorized for distribution by Artak Harutyunyan and Hiroko Oura

July 2024

ABSTRACT: The study provides forward-looking estimates for economic damages from floods and tropical cyclones (TC) for a wide range of countries using global datasets. Damages are estimated for three Intergovernmental Panel on Climate Change (IPCC) scenarios and aggregated at the country level, building them from geographically disaggregated estimates of hazard severity and economic exposures across 183 countries. The results show that, for most countries, floods and TC's damage rates increase (i) during the estimation span of 2020 to 2100, and (ii) with more severe global warming scenarios. In line with other global studies, expected floods and TCs damages are unevenly distributed across the world. The estimates can be used for a wide range of applications, as damage rates represent the key variable connecting climate scenarios to economics and financial sector risk analysis.

RECOMMENDED CITATION: Michele Fornino, Mahmut Kutlukaya, Caterina Lepore, and Javier Uruñuela López. 2024. "A Multi-Country Study of Forward-Looking Economic Losses from Floods and Tropical Cyclones." IMF Working Paper, 24/141.

JEL Classification Numbers:	Q51, Q54, Q56.
Keywords:	Climate change, Forward-looking climate projections, Climate scenario analysis, Economic losses, Damage functions, Tropical Cyclones, Floods.
Author's E-Mail Address:	MFornino@imf.org, MKutlukaya@imf.org, CLepore@imf.org, JUrunuelaLopez@imf.org

WORKING PAPERS

A Multi-Country Study of Forward-Looking Economic Losses from Floods and Tropical Cyclones

Prepared by Michele Fornino, Mahmut Kutlukaya, Caterina Lepore and Javier Uruñuela López[1]

[1] The author(s) would like to thank Hiroko Oura, Artak Harutyunyan, Ivo Krznar, Padma Hurree-Gobin, Henk Jan Reinders, Mehdi Benatiya Andaloussi, Gregor Schwerhoff, Emanuele Massetti, Divya Kirti and Jens Mehrhoff for useful feedback and discussions.

Contents

1. Introduction

The frequency and intensity of natural hazards have increased across several regions in the world since 1950s (Arias and others, 2021). These hazards can cause large economic losses. On a global level, economic loss associated with natural hazards has averaged around $170 billion per year over the past decade, with peaks of $300 billion in some years (UNDRR, 2022). Further, economic losses from these events have risen significantly since the 2000s, in line with their amplified intensity and frequency (UNDRR, 2022). As many countries prepare measures to reduce risks from these natural hazards, it becomes of first order importance to assess future economic losses from the latter under various climate scenarios.[1]

This paper aims to bridge the gap between economic and climate literature by adopting a simple framework for analyzing losses from floods and tropical cyclones (TCs) on a forward-looking basis. We propose a methodology to estimate economic losses from natural hazards that can be applied to a wide range of countries globally.[2] We apply the methodology to estimate forward-looking losses from (riverine and coastal) floods and TCs for a large number of IMF member countries (183 for floods and 89 for TCs) under three Intergovernmental Panel on Climate Change (IPCC) scenarios.[3]

Damages arise as the interaction of three components: the projections of individual hazards (hazard severity), the exposure of economic assets to these hazards, and their resulting vulnerability in the event the hazard materializes. We rely on global datasets for each of these components, with the goal to maximize the coverage of IMF member countries. In terms of hazards, we focus on floods and TCs and used data procured from the private vendor Jupiter Intelligence.[4] Jupiter Intelligence leverages data from various Global Circulation Models (GCMs), as well as additional proprietary models based on recent academic literature, to produce forward-looking measures of hazards' severity under three IPCC scenarios, combination of Shared Socioeconomic Pathways (SSP) and Representative Concentration Pathways (RCP), representing low (SSP1-2.6), intermediate (SSP2-4.5) and very high (SSP5-8.5) Greenhouse Gas (GHG) emission scenarios.[5] For exposures, we use publicly available datasets on spatially disaggregated GDP with global coverage as a proxy for the distribution of physical assets, which is consistent with future socio-economic projections, available decennially up to 2100. To measure vulnerability, we adopt damage functions from existing academic studies and publicly available datasets which translate the magnitude of hazards into quantifiable damages. Specifically, we selected damage functions from Huizinga and others (2017) for floods and Eberenz and others (2021) for TCs. These functions are widely used in the literature, publicly available and provide globally consistent coverage. By merging these three datasets we compute damage rates from floods

[1] For example, we refer to Duenwald and others (2022) for a discussion of the importance of climate adaptation strategies for the Middle East and Central Asia region.

[2] The terms *losses* and *damages* are used interchangeably in this paper.

[3] Floods considered in this study include river and coastal floods, but not rainfall-induced flooding, given data availability (see Section 3.1).

[4] The literature and data on vulnerability and damages from other hazards, such as droughts and wildfires, are still limited especially at global scale, therefore, this study focuses on floods and tropical cyclones only.

[5] The IPCC scenarios have two components: an SSP, which describes how socioeconomic factors may change over the next century, and an RCP, which describes the levels of greenhouse gases and other radiative forcings. They are commonly referred to by the SSP and the RCP components; specifically, the combinations correspond to SSP1 RCP 2.6, SSP2 RCP 4.5, and SSP5 RCP 8.5. Hazards data under SSP 1 RCP 1.9 and SSP3 RCP 7.0 are not readily available.

and TCs for specific locations of interest (specified by latitude and longitude) which are then aggregated to obtain expected annual damage rates at country level.[6]

Our results point to three key takeaways from the analysis. First, most countries we consider will experience an increase in floods and tropical cyclones damages by mid-century. These countries represent a significant share of the global economy. Second, for most countries considered, damages are higher for more severe climate scenarios, pointing to a positive correlation between global flood and tropical cyclones risks and global warming. Third, floods and tropical cyclones risks are unevenly distributed across the world. We now describe the results in more details.

For floods, results show increasing forward looking country-level annual damage rates for most countries (representing 74-80 percent of global GDP in 2020). Depending on the scenario, 58-67 percent of the countries (representing 74-80 percent of global GDP in 2020) display an increase in expected annual country-level damage rate as of 2050 relative to the baseline.[7] Floods risks are widespread across several geographical regions. Countries with the highest damages tend to be in tropical and subtropical areas and have small land area, which makes their assets more geographically concentrated and hence more exposed. The largest relative changes in damage rates are in South America, Africa, and Southeast Asia. Level changes reflect a similar geographical distribution.

For TCs, countries accounting for around 41 percent of 2020 global GDP are expected to experience increased TCs damage rates. Among the countries that are historically exposed to these events, 66-67 percent display an increase in TCs' damage rates from the baseline to 2050. The number of countries with increasing damage rates grows through the years for SSP2-4.5 and SSP5-8.5 and is highest for SSP5-8.5. Looking at the distribution of the damage rates in 2050 and 2100 for the three different scenarios, we observe that the variability of damage rates increases for more severe scenarios at the end of the century for countries with increasing risks. In terms of the geographical distribution of damages, we find that TCs risks are concentrated in specific regions. The countries with the highest damage rates are in the Caribbean, South and Southeast Asia, Eastern Africa, and Oceania.

These results can be used for a wide range of applications, as damages from natural hazards represent the key variable that connects climate physical science to economic and financial sector risk analysis. First, these damages can provide a useful diagnostic tool for climate physical risks in a country. At the moment, available indicators are backward looking and based on data from EM-DAT which are subject to limitations such as missing data and changing trends in climate (Jones and others, 2022).[8,9] Our results provide a forward-looking indicator of floods and TCs risks at country-level based on granular data. Second, as delineated in the IMF staff's approach for climate risk analysis (Adrian, 2022), country-level damages as produced in this paper can be used as an input in macro models to generate macro-financial scenarios accounting for climate physical risks. A macro-financial scenario can then be used to estimate the impact on bank solvency using the standard approach for banks' stress tests. Moreover, the damage or loss component can be integrated directly with borrower-level data, corresponding to a micro approach also described for

[6] We define damage rates as the loss of value of assets, expressed in percent of the value of those assets before being hit by the hazard.

[7] The baseline at country-level is defined in Section 4.

[8] The EM-DAT data are publicly available through the Centre for Research on the Epidemiology of Disasters – CRED website.

[9] Jones and others (2022) provide a detailed missing data diagnosis of the EM-DAT database. The author have identified significant amount of missing data for natural hazards related disasters occurring between 1990 and 2020, specifically on the economic losses.

climate risk analysis. These types of approaches have been used in several IMF Financial Sector Assessment Programs (FSAPs), for example in the Philippines FSAP (Hallegatte and others, 2022), Mexico FSAP (IMF, 2022), and Maldives FSAP (IMF, 2023), to raise awareness of climate risks and to identify pressure points in the financial system. Third, hazard damages can be used to assess mitigation and adaptation strategies. For instance, hazard damages can be used as an input in macroeconomic models to evaluate macroeconomic and financial implications of alternative investment programs and financing strategies.[10]

The rest of the paper is organized as follows. Section 2 provides a review of the relevant literature. Section 3 describes the data adopted for the three components of the framework: hazards, vulnerability and exposures. Section 4 details the methodology adopted to compute losses, starting from damages at a specific location (specified by latitude and longitude) and then aggregating at country-level. Section 5 provides an overview of the key results and the comparison of the results with other studies. Section 6 provides concluding remarks. Annexes contain further information on the data, results, comparison with other estimates and limitations.

2. Literature Review

This study builds on literature aiming to estimate economic losses from climate physical risk, which, while burgeoning in recent years, is still at early stages. Several economic studies have been devoted to chronic risks, in particular the impact of long-term changes in temperature on economic output and growth (e.g., Burke and others, 2015; Kalkuhl and Wenz, 2020; Kahn and others, 2021), while work on acute climate risks has been lagging, with some global estimates for floods from Alfieri and others (2017) and Dottori and others (2018).[11] Botzen and others (2019) provide a review on the estimated direct and indirect economic impacts of natural disasters focusing on the data availability and the range of modeling and empirical approaches implemented.[12]

The direct losses from floods and TCs are the focus of this study. There is a growing literature on indirect losses from hazards which are not reviewed here. We instead focus on direct losses, which are likely to serve as a lower bound of total losses, in relation to individual hazards, as they ignore indirect losses. Further, we focus on two hazards only (floods and TCs). This choice is based on the availability of hazards and vulnerability data.

2.1 Floods

The direct damages from floods mainly depend on the depth of the water. Damage functions for floods link the depth of water to damages—either in percentage of total value or as the absolute damage amount—and can be applied to both types of floods. Even though many different inundation characteristics, like depth, duration, velocity may influence the amount and degree of damage, in the current state-of the-art of flood

[10] For example, the DIGNAD model (Marto et al (2018), Aligishiev et al (2023)) was used to quantify the benefits of enhancing climate-change resilience in the Maldives, (Melina and Santoro, 2021), using an illustrative rather than calibrated shock to capital from natural disasters.

[11] As discussed in Ward and others (2020) the literature on hazards, such as droughts and wildfires, is lagging behind floods and TCs in terms of estimating direct damages and performing forward-looking risk assessments. They note that this is due to the large degree if complexity associated with defining, measuring and analyzing risks from droughts and wildfires. See also Thomas and others (2017), Lüthi and others (2021) and Howard (2014) for wildfires; Cammalleri and others (2020), Lange and others (2020) Ding and others (2011), and Naumann and others (2015) for droughts.

[12] Direct damages are caused by the hazard event itself. Indirect damages do not occur through the event itself but subsequently via connections between system elements as defined by Bachner and others (2023).

damage evaluation mainly inundation depth is incorporated in damage functions as it seems to have the most significant influence.

Several studies in the literature use a multi-model framework, integrating simulations of river flow and flooding processes with datasets on exposures and flood protections to determine damages from floods. Alfieri and others (2017) find: (i) a positive correlation between atmospheric warming and future flood risk at global scale, and (ii) risks are unevenly distributed across the world. Similarly, Dottori and others (2018) analyze socioeconomic costs of river floods, using a multi-model framework. The study finds particularly higher impacts under 3 degrees Celsius warming scenario, with uneven regional distribution. Smith and others (2019) use high-resolution (approx. 30 x 30 m) population density to map flood exposure to population data for 18 countries. The results of the study when compared to other studies suggest that exposure estimates are sensitive to the resolution of the underlying hazard data.

Huizinga and others (2017) estimate empirical damage curves for each continent and asset type, which are now widely used in the literature.[13] To estimate these damage curves, the authors collected a large and globally consistent dataset on flood damages and then produced damage curves providing fractional damage as a function of water depth based on the data. Damage curves are estimated by damage class (residential, commerce, industry, transport, roads, railroads, agriculture) and continent.

Table 1: Global Studies on Economic Losses from Floods

	Year	Coverage	Publicly available damage function	Forward Looking
Huizinga and others	2017	Global – by continent Maximum damage available for 200+ countries	Yes	No
Smith and others	2019	18 developing countries	Yes	No
Alfieri and others	2017	Global	Based on Huizinga and others (2017)	Yes
Dottori and others	2018	Global	Based on Huizinga and others (2017)	Yes

Note: Studies focusing on a single country are excluded.

This paper provides forward looking damage estimates for floods under three different IPCC scenarios by applying damage functions from Huizinga and others (2017). Damage rates, and levels and relative changes under different climate scenarios are provided for 183 countries. While Alfieri and others (2017) and Dottori and others (2018) also provide estimates of global losses, they focus on one scenario (RCP 8.5) and consider a simulated event approach with constant exposures. By contrast, we consider three scenarios as well as time and scenario dependent exposures.

[13] These damage functions are available on the JRC website. These functions have also been used by the NGFS. See, Bertram and others, 2021.

2.2 Tropical Cyclones

TCs typically inflict damage due to strong sustained surface winds, storm surge-driven inundation, and torrential rain. The maximum sustained windspeed is the most important factor to quantify the impact of TCs, also used as an input to damage functions for the assessment of direct economic damage (Emanuel (2011), Czajkowski and Done (2014)).

A large part of the literature on TCs damages focused on the United States. For the United States, damage functions are available for different building types (FEMA (2011), Yamin and others (2014)), as well as for aggregate economic losses for several regions of the U.S. Atlantic and Gulf Coasts (Hallegatte, 2007).

The literature on TCs with global coverage is expanding. Yamin and others (2014) conduct a risk assessment for around 200 countries on TCs. Damage functions are obtained from the HAZUS MH 2.1 Hurricane Model, however, calibrated only for the USA and consider building type and characteristics.[14] Mendelsohn and others (2012) studies global TC damages using an integrated assessment model based on USA's elasticity of damages with respect to storm intensity to calibrate the global damage function. Bakkensen and Mendelsohn (2019) address this modelling drawback, by broadening the damage estimates for a larger set of countries using both a cross-sectional model and an error components model with country and time fixed effects to calculate damage functions. This study shows that the United States is an outlier in TC vulnerability (i.e., much higher elasticities), conditional on its income levels and exposure, hence the risk of overestimating losses when using USA-based damage functions for other countries. Gettelman and others (2017) adopted the TC damage model from the open-source natural catastrophe modelling tool CLIMate ADAptation (CLIMADA)[15] using spatially disaggregated GDP to estimate the impact of future changes in TCs on damages. Authors find increasing global storm damage by around 50 percent in 2070 in comparison to 2015, despite decreasing storm numbers in the future and strong landfalling storms increase in East Asia.

Eberenz and others (2021) developed regionally calibrated damage functions by comparing simulated damages to historical reported damages. Reported damage estimates used in the study are available from the International Disasters Database (EM-DAT). For the regional calibration of the TCs impact model, distinct calibration regions were defined based on geography, data availability, and patterns in damage ratios.[16] The impact functions provided by the study feature considerable differences in the slope and level of uncertainty across model regions. Authors note the largest uncertainties for the North-West Pacific regions.

Table 2: Global Studies on Economic Losses from Tropical Cyclones

	Year	Coverage	Publicly available damage function	Forward Looking
Yamin and others	2014	Global	No – based on damage functions calibrated for the USA	No
Mendelsohn and others	2012	Elasticities based on the USA data.	Yes	Yes

[14] HAZUS is a multi-hazard loss estimation methodology developed by the Federal Emergency Management Agency (FEMA, 2011).
[15] The CLIMADA cyclone damage model produces damage estimates by year and spatial location based on a set of probabilistic cyclone tracks.
[16] These functions are also used by the NGFS.

Bakkensen and Mendelsohn	2019	Global – 87 countries that report damage from TCs	No	No
Eberenz and others	2021	Global	Yes – with regionally calibrated damage functions	No
Gettelman and others	2017	Global – 73 countries	No – Results calibrated to the USA data	Yes

Note: Studies focusing on a single country are excluded.

This paper provides forward looking damage estimates for TCs under three different IPCC scenarios by applying damage functions from Eberenz and others (2021). Damage rates, and levels and relative changes under different climate scenarios are calculated for 89 countries that are exposed to TCs damage.

3. Data

Damages from physical risks arise as the interaction of three components: hazard, vulnerability and exposure. In this section we discuss the data used to quantify each of these components.

3.1 Hazard data

In this study, we used hazard data for floods and TCs severity supplied by the private vendor Jupiter Intelligence.[17] For floods, data covers river and coastal flood depth projections under different scenarios, using data from GCMs as an input.[18] The Jupiter Intelligence's inland river flooding model uses projected regional changes in extreme streamflow to estimate how flood depth and extent may change in a future climate. For coastal floods, multiple climate projection datasets are used to estimate the effects of sea-level rise and storm surge and tides on coastal inundation, as well as storm surge and lake levels on lake shoreline inundation. Values of sea-level rise, long-term lake levels and surge and tides from the same climate scenario are combined to produce a unified estimate of the expected water levels for each scenario. Then river and coastal floods results are consolidated into a single estimate. For TCs, hazards data reflect wind speeds, defined as the maximum 1-minute sustained wind speed at 10 meters above ground level. This measure is produced using data from GCMs and a synthetic TCs model.[19] The maximum 1-minute sustained windspeed variable from the vendor dataset is used in the damages' calculation only for areas where TCs have been observed historically (Figure 1). This approach guarantees consistency between the methodology on the hazards and vulnerability.

[17] Jupiter provides data for some other hazards, including wildfires and droughts. The dataset on hazards projections includes global data for 100,000 locations (latitude and longitude) from Jupiter Intelligence. The locations were selected to maximize global and country-level Gross Domestic Product (GDP) coverage, using the "gridded GDP" projections under SSP2-4.5 by (Murakami and others, 2021). Selected locations provide a coverage of 97 percent of global GDP in year 2040. The location selected within each grid corresponds to the location with highest population within the grid, when available, or the location with the highest GDP. We note that while for some highly localized hazards, e.g., floods, the data for additional locations would add value, for others like tropical cyclones coverage is sufficient considering the underlying resolution of the available hazards data. Additional details are provided in Annex I.

[18] Rainfall-induced flooding is currently not available.

[19] Data include air temperature throughout the lower atmosphere, humidity throughout the lower atmosphere, wind speeds and directions throughout the lower atmosphere, sea- and skin-surface temperatures, surface (sea-level) pressure. Note that multiple GCMs are used from both CMIP5 and CMIP6. Finally, Synthetic TCs tracks can be generated by models based on the physical mechanisms which drive hurricane tracks and intensity. Synthetic tracks can be used to overcome spatial and temporal limitations of historical data.

We use data for the mean levels for flood depth and wind speed, for 10, 20, 50,100, 200, and 500-year return periods. The data also covers fraction of land flooded in 3 arcseconds grids for 10, 20, 50,100, 200, and 500-year return periods.[20] These measures are provided for a baseline (climate for 10-year period centered on 1995) and projections from 2020-2100 with 5-year increments under three scenarios: SSP1-2.6, SSP2-4.5, and SSP5-8.5, which represent a low, intermediate and very high GHG emission scenario respectively.[21] The three scenarios are drawn from the IPCC Sixth Assessment Report (IPCC, 2021). As an example, Figure 2 shows flood depth for 1-in-500-year return period in 2050 under the scenario SSP2 4.5.

Figure 1: Tropical Cyclones grids

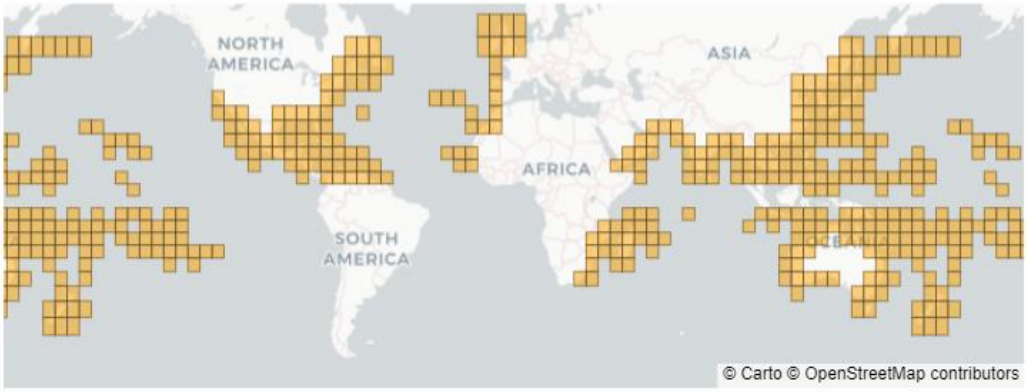

Source: Jupiter Intelligence. Notes: Grids that consider TC simulations in wind parameter estimates from Jupiter Intelligence

Figure 2: Jupiter Intelligence flood depth

flood depth in meters

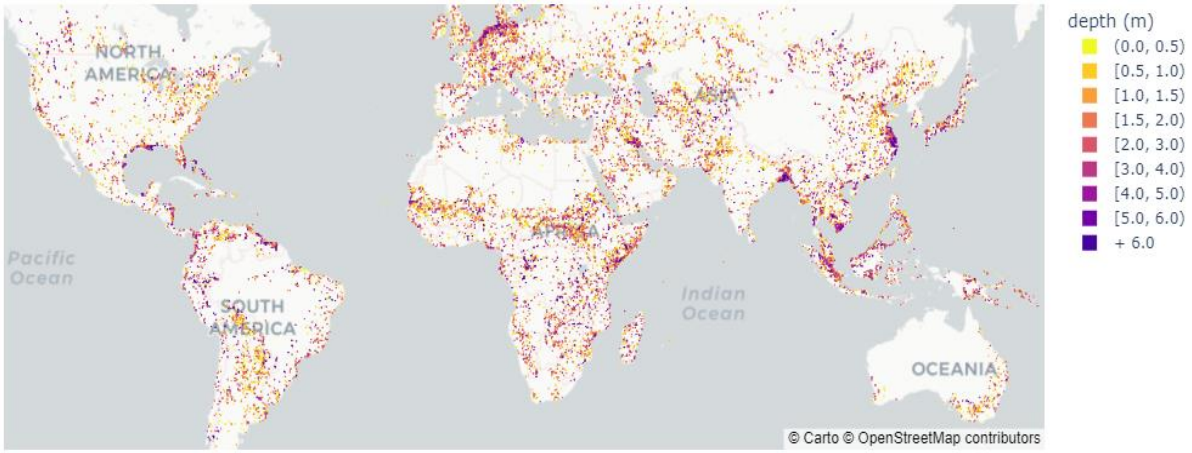

Source: Jupiter Intelligence. Notes: Values for mean depth meters for 1-in-500 year in 2050 under SSP2-4.5

[20] An arcsecond is a second of arc i.e. $\frac{1}{60}$ of an arcminute which is a unit of angular measurement equal to $\frac{1}{60}$ of one degree. A degree is a measurement of a plane angle in which one full rotation is 360 degrees. At the equator, an arcsecond of longitude approximately equals an arcsecond of latitude which is approximately 30 meters.

[21] We note that the SSP5 - 8.5 represents an extreme scenario, and its plausibility is currently debated in the literature. However, as noted in (IPCC, 2023), this scenario cannot be ruled out. Furthermore, for some of the potential applications of our results, such as financial sector stress testing analysis, it is important to adopt extreme scenarios to analyze the potential implications of tail risk events.

3.2 Vulnerability – Damage functions

Damage functions relate economic damages to climate inputs. Hazards can be linked to economic and financial exposures using damage functions that define the impacts of specific hazards on real assets and activities (BIS, 2021). These functions can be estimated using different methodologies, including by using empirical approaches looking at correlative relationship between past data on damages and hazards variables and using simulated data of physical hazards and models to explicitly describe the system behavior in response to climate change (Feyen and others 2020). Damage functions vary by hazard, type, and geographical location (e.g., regions, continents, or countries) of exposures. This granularity is intended to capture differences in the way in which a climate hazard of the same intensity differently impacts physical assets at different locations–for example because of different climate resilience of existing infrastructure. We selected the functions estimated by Huizinga and others (2017) and Eberenz and others (2021), as they are widely used, publicly available and provide globally consistent coverage.

The damage functions provided by Huizinga and others (2017) can be used to calculate damages from floods. These functions are piecewise linear, depicting fractional damage as a function of water depth for a variety of categories: buildings and contents (residential, commercial, and industrial), transport facilities, infrastructure (roads and railroads) and agriculture (Figure 3). The functions have been calibrated using quantitative data from multiple studies. Damage functions vary also by geography, they are calibrated for six continents: Europe, Africa, Asia, Oceania, North America, South and Central America.[22]

Figure 3: Floods damage functions by asset type

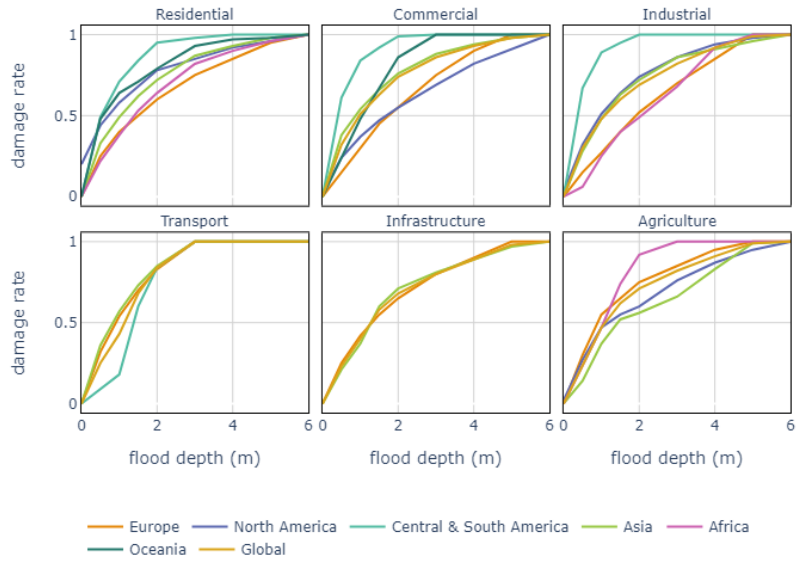

Source: Huizinga and others (2017)

[22] As noted by the authors the amount of historical data in which acute events are properly recorded is larger for the countries and continents with a more established systematic damage assessment 'tradition', like the USA, Australia, Japan and South Africa. However, and specifically in the African continent (except South Africa), the information available is not equally distributed over the continent and mostly available for sub-Saharan Africa.

The damage functions provided by Eberenz and others (2017) are calibrated for the assessment of economic damages caused by TCs. These functions are regionally calibrated (Figure 4) by using simulated damages from CLIMADA and reported damages. The functional form is sigmoidal, expressing the percentage of damage as a function of wind speed:

$$f = \frac{v_n^3}{1 + v_n^3},$$

where

$$v_n = \frac{MAX[(V - V_{thresh}),0]}{V_{half} - V_{thresh}}.$$

In this formula, V is the 1 min sustained wind speed at 10 m above ground per storm event. V_{thresh} is a minimum threshold for the occurrence of impacts, as no directly wind-induced damage is expected for low wind speeds. V_{half} is the slope parameter, signifies the wind speed at which the function's slope is the steepest and the impact reaches 50 percent of the exposed asset value. This functional form, introduced by Emanuel (2011), builds on empirical studies relating wind to damage suggesting a high power-law dependence of damage on wind speed (Pielke 2007). Emanuel (2011) argues that on physical grounds damage should vary as the cube of the wind speed over a threshold value. Further, the fraction of the property damaged should approach unity at very high wind speeds.

Figure 4. Calibrated TC Damage Functions by Regions

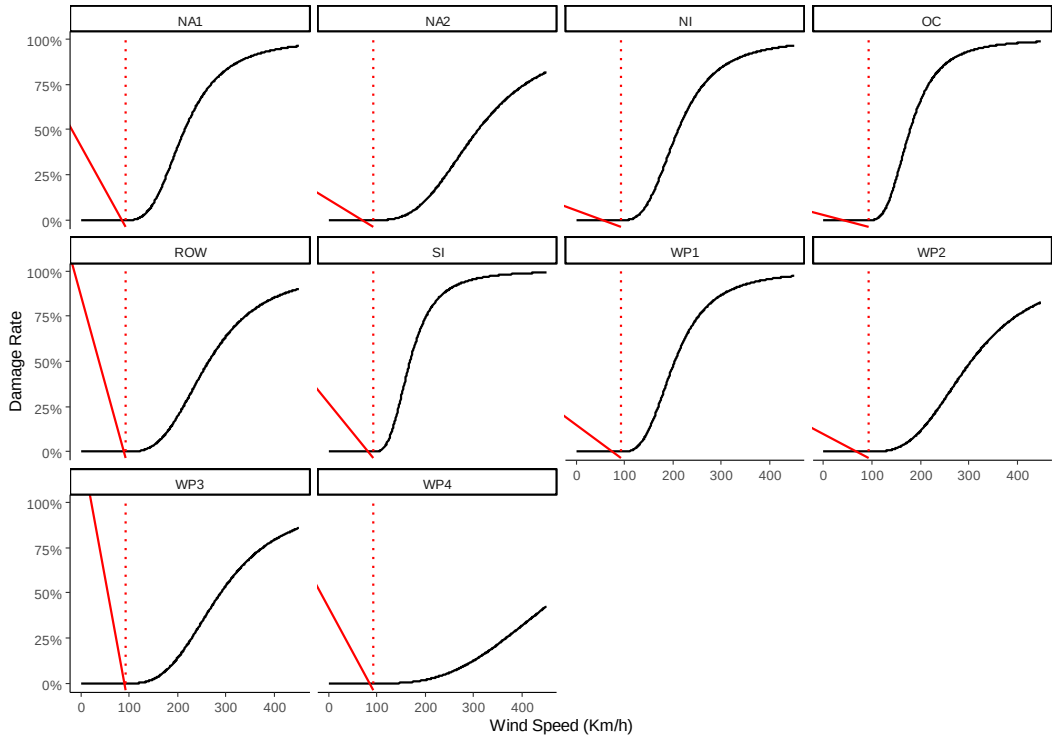

Source: Eberenz and others (2021)

Notes: The red dotted line represents a windspeed of 25.7 m/s, or 92.5 km/h, which is the threshold below which the damage rate is assumed to be zero. Regional groupings are defined in detail in appendix Table A.1 of Eberenz at al (2021), p.409. For reference, NA=North Atlantic, NI=North Indian, OC=Oceania, ROW=Rest of the World, SI=South Indian, WP=North West Pacific. Numbers denote sub-regional groupings of countries that share similar characteristics. NA2=CAN, USA, WP2=PHL, WP3=CHN, WP4=HKG, KOR.

3.3 Exposures

We proxy economic exposures using downscaled GDP data. Several studies have developed methodologies to downscale national or subnational GDP data into finer spatial units, combining it with other auxiliary datasets (such as population data). In these datasets, each GDP value has an associated latitude and longitude, which corresponds to the centroid of the corresponding geographical grid cell. In particular, Murakami and others (2021) develop a downscaling methodology to estimate gridded GDP under different SSPs, which we use in our analysis. Details of the downscaling approach are provided in Annex II.

The global dataset of downscaled GDP data at 30 arcminutes is publicly available. The dataset spans between 1980 and 2100 by 10-year intervals. The data between 1980–2010 are estimated by downscaling actual GDPs by country, while those between 2020–2100 are estimated by downscaling projected GDPs under three SSPs (SSP1-2.6; SSP2-4.5; and SSP5-8.5). Figure 5 illustrates Gridded GDP under SSP2-4.5 scenario for 2050.

Figure 5: Gridded GDP SSP2-4.5 for 2050

GDP PPP 2005, Million USD

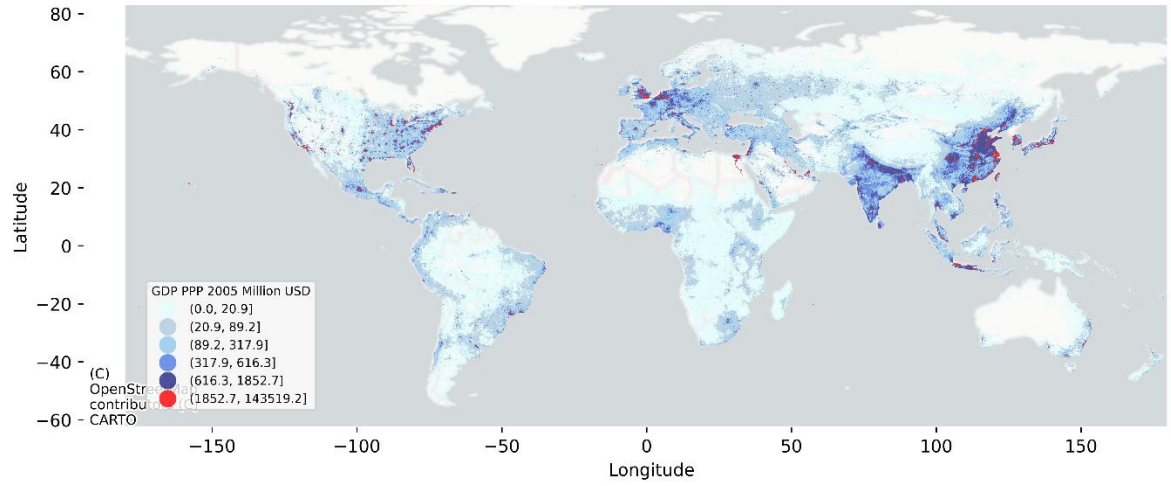

Source: Murakami and others (2021)

Notes: GDP groupings have been defined using the following percentiles [0, 50, 75, 90, 95, 99, 100]

4. Methodology

This section provides the methodology adopted to estimate damages. We focus on direct damages and exclude indirect damages, for example, arising from business interruption, spillovers, and, more generally, second round effects. We define damage rates as the loss of value of assets, expressed in percent of the value of those assets before being hit by the hazard. Damage rates from floods and TCs are calculated separately. Caution should be applied if interested in combining damages from both floods and TCs, as these events are likely to be correlated, for example, with TCs possibly leading to flooding. In this section, we describe how damage rates for a specific location (given by latitude and longitude) are computed and we detail how location-level damage rates are used to calculate aggregate damage rates at the country level. The methodology can be applied for different projection horizons and scenarios, as depicted in Section 5.

4.1 Location-level damage rate

The calculation of the damage rate at the individual location requires applying the damage function to the hazard data for that point. The variables $depth_{c,i,RP,t,s}$, $frac_{c,i,RP,t,s}$, and $wind_{c,i,RP,t,s}$ denote the flood depth, fraction of land flooded, maximum sustained windspeed respectively in country c, location i, return period RP, projection year t and scenario s. The RP denotes the return period at which specified hazard intensity is expected; for example, the 1-10 years flood depth denotes the severity of a hazard that is expected to occur no more than once in 10 years.[23] Next, we denote the damage function for floods as df_{floods} and the damage function for TCs as df_{storms}. These functions take as inputs either the flood depth or the maximum sustained windspeed and return the fraction of assets that are lost as a result.

For floods, the specific damage function depends on the percentage of built-up area in the location. For each covered cell in the gridded dataset, we divide the exposure measure into built-up and non-built-up areas using the land cover data Copernicus Global Land Operations "Vegetation and Energy" (CGLOPS-1) for 2019 from Buchhorn and others (2020).[24] At the time of the analysis, this was among the few publicly available datasets that cover built-up areas, but this data is rapidly evolving and further granularity can be integrated in the future.[25] For built-up areas, we combine the residential, commercial, and industrial damage functions (Figure 3), by equally weighting each function, while for non-built-up areas we consider agriculture and infrastructure damage functions. For TCs the damage function differs by country groups (Figure 4).

The damage rate for floods is defined as:

$$d_{c,i,RP_j,t,s} = frac_{c,i,RP_j,t,s} * df_{floods}(depth_{c,i,RP_j,t,s}).$$

The damage rate for TCs is defined as:

$$d_{c,i,RP_j,t,s} = df_{storms}(wind_{c,i,RP_j,t,s}).$$

Expected annual damage rate can be calculated using the damage rates for different return periods for a given location. Hazard data are available for 10, 20, 50,100, 200 and 500-year return periods, which are denoted as $RP_{10}, RP_{20}, RP_{50}, RP_{100}, RP_{200}, RP_{500}$. The trapezoidal rule is used to approximate the area under the damage-return curve (Figure 6).

[23] The return period is the inverse of the probability of that flood depth or wind level being exceeded in a year. It is common practice to provide hazard severity data for specific return periods and to use the data to estimate the average expected damage per year.
[24] Copernicus Global Land Operations "Vegetation and Energy" (CGLOPS-1) for 2019 from Buchhorn and others (2020) offer different land cover datasets at approximately 100 meter at the equator. The land cover datasets provide geospatial information on the physical coverage of the earth's surface as discrete classification products, classifying each grid into a single category, and cover fractions, also referred to as fraction cover layers, which describe what fraction of the grid is covered by a specific category. Specifically, we adopt the BuiltUp-CoverFraction-layer at 100 m resolution. To match the resolution from the Built-up-CoverFraction-layer to that of the gridded GDP, we performed an average down sampling to upscale the Built-up-CoverFraction-layer to 5 arcminutes resolution. The average down-sampling considers a weighted average of all non-NA contributing pixels, i.e., all initial resolution centroids contained in the 5 arcminutes grid.
[25] GHSL - Global Human Settlement Layer: GHS-BUILT-S R2023A - GHS built-up surface grid, derived from Sentinel2 composite and Landsat, multitemporal (1975-2030), became available in 2023, providing total built-up surface and the built-up surface allocated to dominant non-residential.

Figure 6: Damage-probability curve

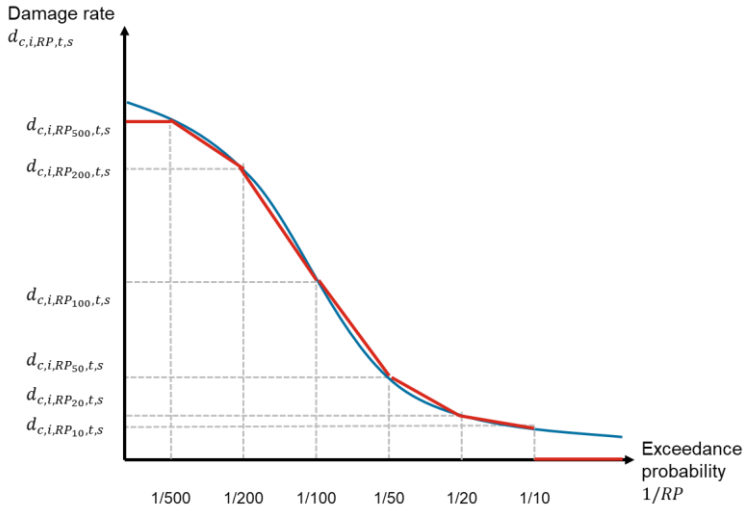

Source: IMF staff calculations

For floods and TCs, the discretized random variable $d_{c,i,t,s}$, with severity measure $sev_{c,i,t,s} \geq 0$, is defined as follows:

$$d_{c,i,t,s} = \begin{cases} 0, if\ sev_{c,i,t,s} < sev_{c,i,RP_{10},t,s} \\ \frac{d_{c,i,RP_j,t,s} + d_{c,i,RP_{j+1},t,s}}{2}, \quad if\ sev_{c,i,RP_j,t,s} \leq sev_{c,i,t,s} < sev_{c,i,RP_{j+1},t,s} \\ d_{c,i,RP_{500},t,s}, \quad if\ sev_{c,i,t,s} \geq sev_{c,i,RP_{500},t,s} \end{cases}$$

where $j \in \overline{RP} = \{10,20,50,100,200,500\}$. In turn, the location-level expected annual damage rate can be calculated as:

$$E[d_{c,i,t,s}] = \sum_{j \in \overline{RP}} \left(\frac{1}{RP_j} - \frac{1}{RP_{j+1}}\right)\left(\frac{d_{c,i,RP_j,t,s} + d_{c,i,RP_{j+1},t,s}}{2}\right) + \frac{d_{c,i,RP_{500},t,s}}{RP_{500}}.$$

4.2 Country-level expected damage rate

Damage rates for specific locations in a country are aggregated to obtain country-level damage rates, which incorporate both hazard and exposure factors. We consider all locations $i = \{1, \dots, n\}$ in a country c for which we have hazard data, so that n represents the number of cells considered in country c. We denote the gridded GDP at a location as $GDP_{c,i,t,s}$, and the total GDP of the country as $GDP_{c,t,s}$. We define the country-level expected damage rate for a specific year and scenario, denoted with $E[D_{c,t,s}]$, as the weighted average of the location-level expected damage rates, where the weight of a location is given by its GDP:

$$E[D_{c,t,s}] = \sum_{i=1}^{n} E[d_{c,i,t,s}] \frac{GDP_{c,i,t,s}}{GDP_{c,t,s}}$$

Key results of the paper in the next section focus on the country-level expected damage rate by time and scenarios, hereafter referred to as damage rate for simplicity. Results are also presented in terms of the change in levels and relative change of the damage rate in a given year and scenario relative to the historical baseline, which represents the hazard for the 10-year period centered around 1995 and GDP in 2000. These are defined, respectively, as

$$E[D_{c,t,s}] - E[D_c](\text{baseline})$$

and

$$(E[D_{c,t,s}]/E[D_c](\text{baseline})) - 1.$$

These variables provide information on whether and how flood and TCs risks are expected to change in the future, as well as how these changes vary depending on the scenario considered.

5. Results

This section discusses floods and TCs damages, respectively, and compares results with other studies. We selected 2050 and 2100 as projection horizons to showcase our results. The year 2050 is important for convergence to net zero in time to successfully mitigate global warming, while 2100 is the furthest year available in the sample at our disposal.

5.1 Floods damages

Flood risks are projected to increase for most countries by mid-century. Depending on the scenario considered, 58-67 percent of the countries (representing 74-80 percent of global GDP in 2020) display an increase in the country-level expected damage rate in 2050 relative to the baseline (Table 3). The median damage rate for these countries is 0.28-0.35 percent in 2050 and 0.36-0.41 percent in 2100 depending on the scenario. For the remaining countries, 25-33 percent (representing 18-25 percent of global GDP in 2020) display a decrease in flood risks, and the rest display no change. The median damage rate for these countries is 0.22-0.32 percent in 2050 and 0.25-0.27 percent in 2100 depending on the scenario. The number of countries with rising flood risks increases over time and with global warming, being highest under the SSP5-8.5 scenario.

Table 3: Key statistics for flood damages

Time	Scenarios	# of countries (median country-level damage rate in percent) with increasing flood risks	# of countries (median country-level damage rate in percent) with decreasing flood risks
2050	SSP1-2.6	107 (0.35)	60 (0.22)
	SSP2-4.5	115 (0.28)	52 (0.32)
	SSP5-8.5	123 (0.32)	45 (0.32)
2100	SSP1-2.6	121 (0.36)	47 (0.26)
	SSP2-4.5	117 (0.36)	51 (0.27)
	SSP5-8.5	124 (0.41)	44 (0.25)

The variability of damage rates increases for more severe scenarios at the end of the century for countries with increasing risks. Figure 7 shows the distribution of damage rates, conditional on the damage rate increasing (LHS) or decreasing (RHS) relative to the baseline year**.** The number of extreme observations increases as well. Most of these are countries characterized by having a small land area, and hence more concentrated flood risks and economic activity, such as small island countries. The distribution of damage rates for countries with decreasing damage rates is more stable across time and scenarios, with the extreme observations scattered in various regions.

Figure 7: Floods' damage rates for countries with increasing (left-hand panel) and decreasing (right-hand panel) damages relative to the baseline.

In percent

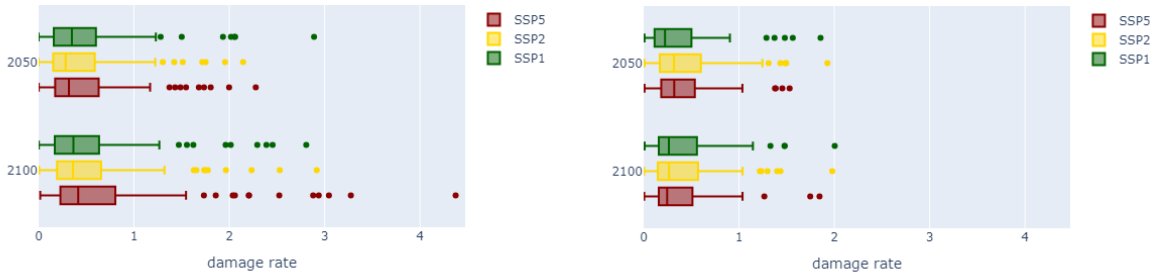

Source: IMF staff calculations

In line with other global studies (Alfieri and others 2017; Dottori and others 2018) we find that floods risks are unevenly distributed across the world. We focus our attention to the SSP2-4.5 scenario, which represents an intermediate emissions scenario. Similar general findings hold for the other scenarios SSP1-2.6 and SSP5-8.5, representing a low and very high greenhouse gas emission scenarios.[26] We find that the countries among the top 10 with the largest damage rates in the three scenarios are in different geographical regions, mostly in tropical and sub-tropical regions, and most have a small land area.

Figure 8: Floods' damage rate for 2050 under SSP2-4.5

In percent

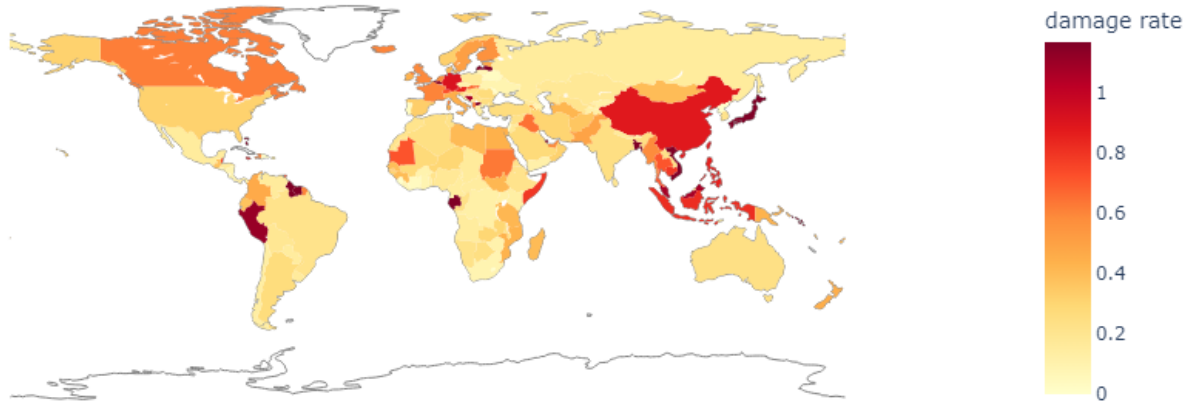

Source: IMF staff calculations

[26] The results are available in Annex V.

Several countries experience significant relative increases in floods' damages already by 2050, relative to the baseline, as well as by the end of the century. The relative changes have a median of 8.46 and 17.37 percent by 2050 and 2100, respectively. The largest relative changes in damage rates are in South America, Africa, and Southeast Asia. The changes in levels reflect a similar geographical distribution but are generally small, with a median of 0.02 percentage points in 2050 and 0.03 in 2100. It is important to consider all these three metrics together when assessing flood risks for a specific country to have a complete picture.

Figure 9: Floods' damage rate relative and levels change between the baseline and 2050 under SSP2-4.5

Relative change
In percent

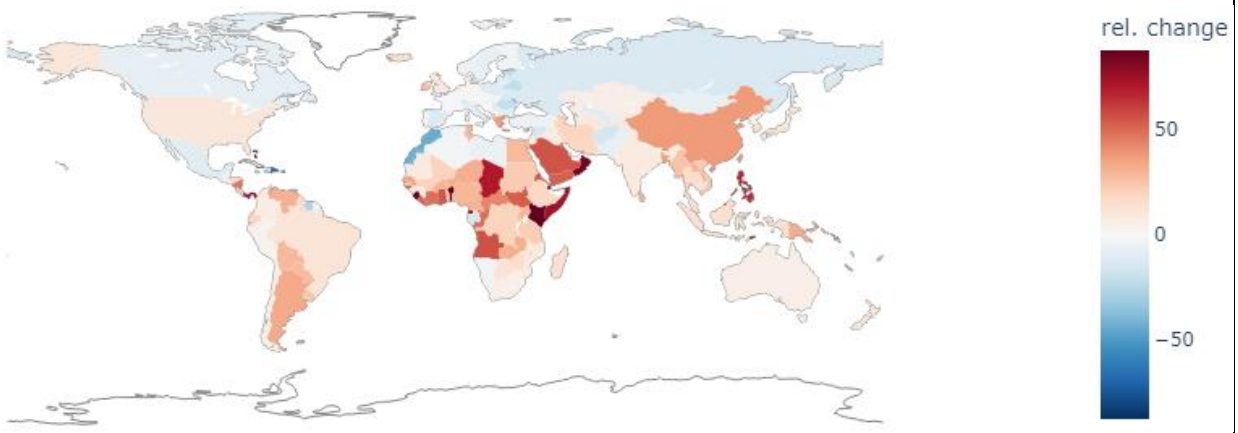

Levels change
Percentage points

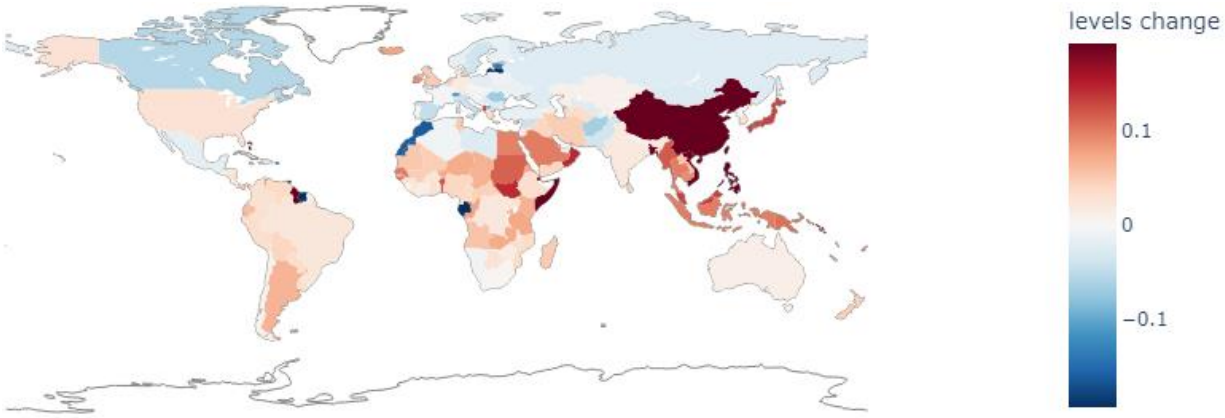

Source: IMF staff calculations

Country-level damage rate changes over time and scenarios are mainly driven by corresponding changes of the hazard severity (flood depth). For most countries damage rates increase over time and as we consider more severe scenarios. An important driver of this findings is the change in (average) flood depth over time, which displays generally increasing trends across time and scenarios. However, certain regions of the world including in high-latitude regions such as Canada and some parts of Europe, are expected to

experience drier climates which can lead to a decrease in riverine floods risks.[27] More details on the drivers of floods hazard damages are provided in Annex III.

5.2 Tropical cyclones damages

Most countries historically exposed to TCs will see an increase in damages associated to TCs in future decades (Table 4). We calculate projected damages from TCs for 89 countries that are in regions where such events are in the historical record. Depending on the scenario, 66-67 percent of the exposed countries (with the exposed areas representing 40-42 percent of global GDP in 2020) display an increase in country-level expected damage rate in 2050 relative to the baseline, with a median damage rate for these countries of 0.11-0.12 percent in 2050 and 0.12-0.16 percent in 2100 depending on the scenario (Table 4).[28] In the sample, 16-17 percent (with exposed areas representing 4-5 percent of global GDP in 2020) display a decrease in TC risks. The number of countries with increasing damage rates is highest for SSP5-8.5.

Table 4: Key statistics for TCs damages

Time	Scenarios	# of countries (median country-level damage rate in percent) with increasing TC risks	# of countries (median country-level damage rate in percent) with decreasing TC risks
2050	SSP1-2.6	59 (0.11)	15 (0.0019)
	SSP2-4.5	60 (0.11)	14 (0.0006)
	SSP5-8.5	59 (0.12)	15 (0.0025)
2100	SSP1-2.6	57 (0.12)	17 (0.0015)
	SSP2-4.5	60 (0.13)	14 (0.0012)
	SSP5-8.5	63 (0.16)	11 (0.0007)

The distributions show that the variability of damage rates increases for more severe scenarios at the end of the century for countries that will see an intensification of risk. In Figure 10, we plot the distribution of damage rates conditional on the damage rate increasing (left-hand panel) or decreasing (right-hand panel) relative to the baseline year. The number of extreme observations is overall stable for countries with increasing and decreasing damage rates. All the extreme values in the Figure 10 (left-hand panel) are island countries; small island countries are among the top five countries by damage rate for 2050 and 2100 in the different scenarios.

[27] While flood risks are expected to decrease for these countries, other hazards such as droughts and wildfires might be increasing. Hence, our results should not be interpreted as physical risks being decreasing overall for these countries.

[28] When only certain parts of a country are exposed to TCs, we account only for the GDP within these grids.

Figure 10: Tropical cyclones' damage rates for countries with increasing (left-hand panel) and decreasing (right-hand panel) damages relative to the baseline

In percent

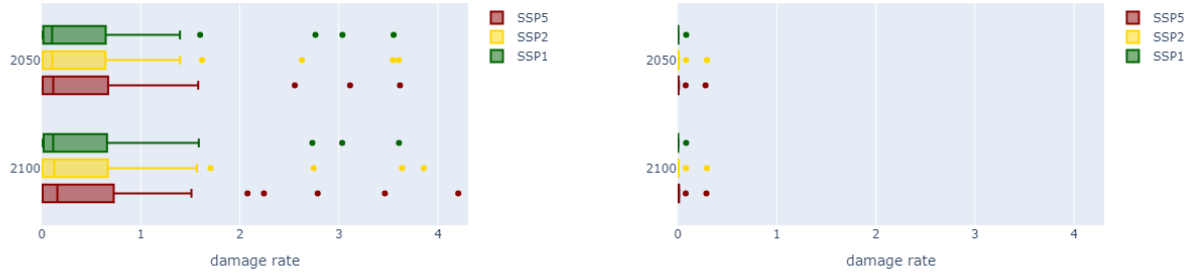

Source: IMF staff calculations

Geographical distribution of TC's damages indicate concentration in certain regions under SSP2-4.5 scenario. Similar general findings hold for the other scenarios SSP1-2.6 and SSP5-8.5.[29] Countries with the highest damage rates are in the Caribbean, South and Southeast Asia, Eastern Africa, and Oceania.

Figure 11: Tropical cyclones' damage rate for 2050 under SSP2-4.5

In percent

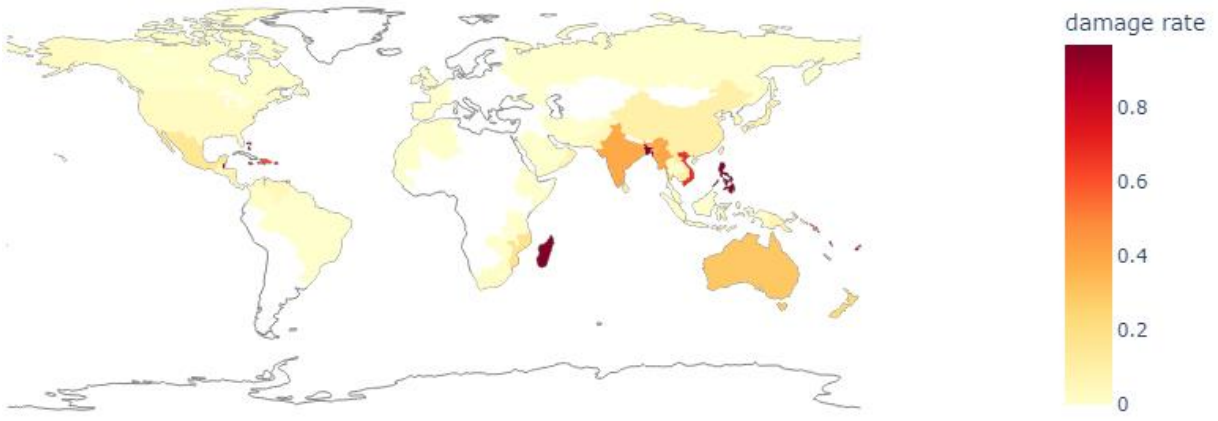

Source: IMF staff calculations

Most countries historically exposed to TCs experience increases in TCs related damage rates. Countries show a relative change median of 6.95 percent by 2050, which reaches 14.20 by the end of the century. North and Central and South America, and countries along the coast from Eastern Africa to Oceania, show the largest changes. High changes in the levels of damage rates are observed in countries in the Caribbean, Southeast Africa, and Southeast Asia. Drivers of TCs hazard damages are provided in Annex IV.

[29] The results are available in Annex VI.

Figure 12: Tropical cyclones' damage rate relative and levels change between the baseline and 2050 under SSP2-4.5

Relative change
In percent

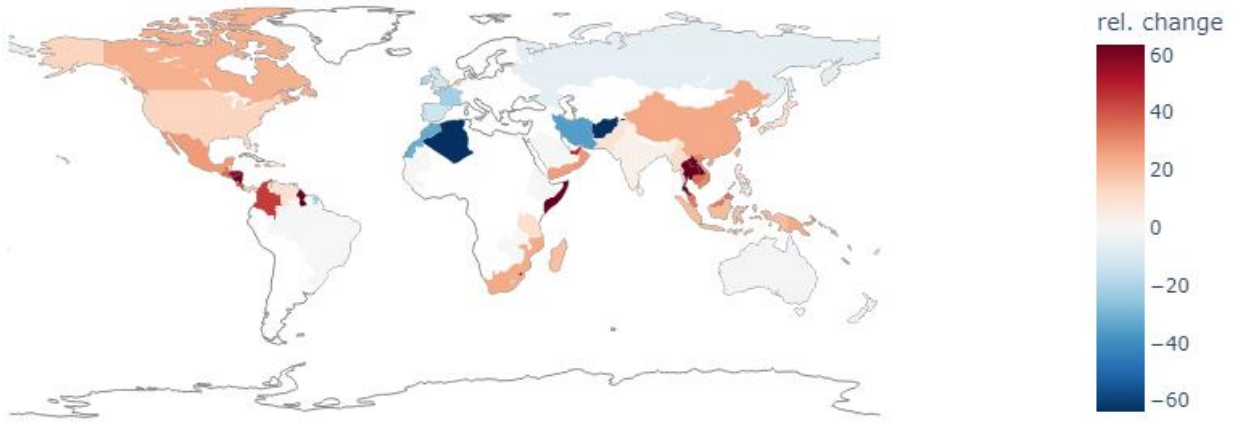

Levels change
Percentage points

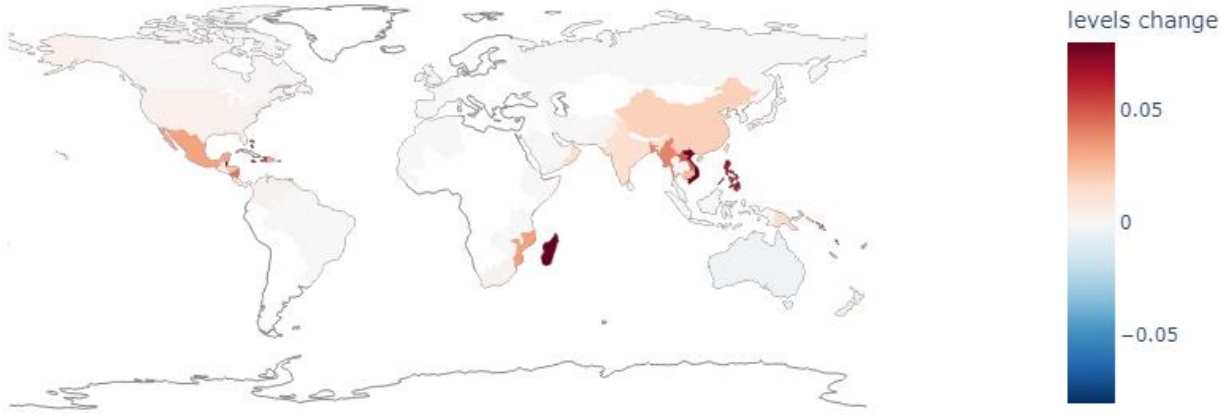

Source: IMF staff calculations

5.3 Comparison of results with other studies and limitations

This section provides a comparison of the results with select studies in the literature, and with estimates produced by the Network for Greening the Financial System (NGFS). In general, the comparison with other studies is challenging due to the differences in inputs, methodologies, time periods and scenarios. Furthermore, uncertainty on the quantification of each component of the methodology is generally large. Annex VIII expands on the discussion of uncertainties related to this study. Regarding the comparison with the forward-looking estimates from NGFS-Phase III, the main challenge arises from the fact that the NGFS outputs are available in relative changes only.[30] With these limitations in mind, we focused on two types of comparisons. First, we benchmarked the magnitudes of our damage rates in 2020 with the historical losses reported in other global studies in the literature. Focusing on 2020 data allows us to abstract from climate scenarios. Second, we compared the sign of the change in our forward-looking damage rates with the ones from the NGFS, whose methodologies and scenarios are closest to ours.

Historical losses are broadly aligned. For floods, global historical losses are available from Dottori and others (2018) which finds estimates of 0.4 percent of global GDP. In our study, the median for all countries is of 0.8 percent of GDP in the baseline.[31] For TCs, historical global annual average damages as a percentage of total asset value from different studies are compiled in Eberenz and others (2021) and range from 0.02 to 0.09.[32] Our global historical estimated losses are 0.06 percent, hence again in a similar range.

The sign of changes in forward-looking damages from the NGFS is the same as ours for more than half of the countries considered. The NGFS integrated acute physical risk damages from TCs and floods in their Phase III scenarios, which we used for comparison. The approach used is similar to the one adopted in this study, but there are differences in the data and methodological approaches, which underpin the differences we find.[33] The details on the NGFS's approach and the comparison exercise are provided in Annex VII. Overall, there is consistency between the estimates for more than half of the countries, and this is true across scenarios and years. To compare results, for a given country we define the results consistent when the relative change in damage rates in our study and NGFS Phase III has the same sign for a specific year and scenario. For floods, the analysis shows that, on average, the results are consistent for 65 percent of the countries (with a maximum of 70 percent and a minimum of 60 percent). We see similar results for TCs, with an average of 55 percent of countries' results being consistent across years and scenarios (a maximum of 57 percent and a minimum of 51 percent).

While our results provide a useful starting point for the analysis of physical risk, there are several important limitations and challenges. For example, hazards projections are subject to uncertainty from the climate modelling and statistical techniques used to produce them. Adaptation measures, which are an important factor, are challenging to measure and as such not explicitly accounted for in this study.[34] Furthermore, this study analyzed floods and TCs damages in isolation. As explained above, combining damage

[30] While this type of output is certainly useful for practitioners, it only allowed us to compare directions but didn't provide useful insights regarding the size of damages.

[31] To make the results comparable we have expressed our results in percentage of GDP, but they still represent asset losses.

[32] The damages considered in Eberenz and others (2021) comes from their own model as well as EM-DAT, GAR (2013) and Gettelman and others (2017), and are based on different time periods spanning from 1950-2014.

[33] Annex VII includes details on the data and methodological approach differences.

[34] Only for floods in the USA, England, the Netherlands and Germany Jupiter assumes that locations protected by levees will be protected up to and including a 100-year flood.

rates from floods and TCs may prove challenging given the likely correlation between these events. Finally, given the wide range of countries covered, we relied on global datasets. When focusing on a single country calibrated data for the specific country might be more useful. A detailed description of limitations is available in Annex VIII.

6. Conclusions

The IMF recently integrated climate change considerations in its work program, as climate change is found to be macro-critical.[35] For example, IMF's surveillance work now routinely includes the impact of climate change on fiscal and monetary policy, while a new climate-related financial instrument, the Resilience and Sustainability Facility, has been recently introduced.[36] The focus on climate change also spotlighted some important data gaps. The IMF's Data Gaps Initiative 3 (DGI-3) aims to bridge policy-related data gaps by developing suitable methodologies to develop adequate data.[37] In particular, recommendation #5 of the DGI-3 focuses on forward looking physical and transition risk indicators to assist policymakers in determining the timing and scope of climate policies.

The damage estimates provided by this study are a step towards closing forward-looking, physical risk-related data gaps. The estimates can be used for cross-country assessments of the importance of certain physical risks (floods and TCs) and connect future climate projections to economic and financial sector risk analysis**.** Nowadays, most of the available estimates are backward looking and often subject to limitations such as missing data. Our results provide forward-looking estimates for floods and TCs risks at country-level based on granular data, expanding the available literature. Finally, as discussed above, these results can be used as inputs to the calibration step of quantitative macroeconomic models that may be used for policy assessments.

Intermediate outputs and the modular structure of our methodology can foster exploring innovative approaches. The location-level damages can be a starting point to explore alternative approaches, such as matching the financial system's geographical exposures to these location damage rates using geospatial techniques and, in this way, to capture the institutions' geographical diversification or concentration. Moreover, the modular approach in the methodology and intermediate outputs provide enough flexibility to refine and adapt to specific needs. Incorporating additional information on any of the three layers (hazards, exposure, and vulnerability) can improve the estimates (e.g., using threshold derived from construction codes specifications) or transform the estimates to country specifics (e.g., changing to an exposure that is more relevant, such as tourism infrastructure for tourism-dependent countries). The range of possibilities goes together with the development of and access to alternative data sources, such as geospatial features from Open Street Maps and Google Maps and satellite imagery from the National Aeronautics and Space Administration and the European Space Agency.

[35] See Kristalina Georgieva's speech available here.

[36] The Resilience and Sustainability Facility (RSF) provides affordable long-term financing to countries undertaking reforms to reduce risks to prospective balance of payments stability, including those related to climate change and pandemic preparedness.

[37] Further details on DGI-3 can be found here.

Annex I: Jupiter Intelligence Data

This annex provides detailed information on how the main hazard variables of interest are constructed by the vendor that the IMF selected for climate physical risk data. As discussed in the main text, Jupiter Intelligence provides forward-looking physical risk projections under SSP1-2.6, SSP2-4.5, SSP5-8.5 climate scenarios, for both a baseline year and 5-year projections from 2020 through 2100. Such projections are the outcome of a rigorous re-elaboration of the output of conventional global climate models, to which Jupiter Intelligence adds proprietary methodologies to downscale and distill quantitative results for individual perils using a variety of statistical and modeling techniques.

River and costal flood depth projections are the two inputs used to calculate the flood depth variable. Jupiter Intelligence's inland river flooding model uses projected regional changes in extreme streamflow to estimate how flood depth and extent may change in a future climate. The primary input for the projections is data (i.e., projected runoff) from several models from the Climate Model Intercomparison Project (CMIP6). A hydro-geomorphological flood modeling technique based on Nardi and others (2006, 2019) is leveraged to obtain flood depth. Relative changes in climate model outputs are then implemented to inform the relative changes in depth under different scenarios. The model uses a hydrologically conditioned digital elevation model. That is, the DEM elevations have been corrected to remove artifacts that could cause errors when simulating the water flow over the terrain. These include several bias-correction augmentations, like resolving erroneous depressions where water would inappropriately pool, correcting flat slopes to ensure water flows correctly, and several other corrections. Finally, depths are expanded across the surrounding topography while preserving hydrologic connectivity, which means that grid points are only affected by flooding in the river channels whose watershed they are in (e.g., Nobre and others, 2011). Historical observations from in-situ river gauges are used to calibrate the statistical relationship at the heart of the hydro-geomorphological model (e.g., Nardi and others, 2019).

For coastal floods, Jupiter Intelligence uses multiple climate projection datasets to estimate the effects of sea-level rise and storm surges/tides on coastal inundation, as well as storm surge and lake levels on lake shoreline inundation. Specifically, for sea-level rise, the Kopp dataset (Kopp and others, 2014) is used, and is adjusted based on recent sea-level rise estimates (Sweet and others, 2017). This adjusted dataset provides estimates of expected sea-level rise at multiple discrete coastal locations globally, as well as projections from multiple scenarios, including uncertainty. For the expected magnitude of storm surge and tides, the Global Tide and Surge Reanalysis (GTSR; Muis and others, 2016) is used to estimate the 100-, 200-, and 500-year return of surge and tide levels historically. GTSR provides daily estimates of historical water levels (surge and tide) globally at several gauge locations and other model-derived coastal points, and Jupiter Intelligence bias-corrects these estimates using observations from NOAA and Global Extreme Sea Level Analysis (GESLA; Woodworth and others, 2016) observational databases. A high-resolution digital elevation model, corrected by Jupiter Intelligence for shortcomings associated with urban areas, is used to estimate the local coastlines. The inland penetration of these water levels is estimated using an algorithm that preserves hydrologic connectivity between inland locations and the coastline (Nobre and others, 2011). The resulting maps of possible flood depth and extent are used to assess flood exposure.

Values of sea-level rise / long-term lake levels and surge/tide from the same climate scenario are combined to produce a unified estimate of the expected water levels for each scenario. Then, Jupiter Intelligence consolidates river and coastal results into a single number, which is the one we rely on for our study.

For TCs, Jupiter Intelligence provides wind speeds, defined as the maximum 1-minute sustained wind speed at 10 meters above ground level, under different scenarios. This measure is produced using data from GCMs and a synthetic TC model. The synthetic model is used to capture the contribution of local extreme winds, which GCMs do not capture, as well as to overcome the limitations of historical data available from International Best Track Archive for Climate Stewardship (IBTrACS). To simulate how storms may be different in future years, a regression-based approach is used to relate TC intensity to variables representing aspects of the surrounding environment.[38] To account for local variations in the response of TCs to environmental conditions, the regression model is calibrated for different regions of the globe. For each period, the maximum near-surface wind speed is collected at each spatial grid point. The data are aggregated to produce an annual maximum series, which is the maximum wind speed value in each year. A probabilistic statistical fit captures the characteristics of wind speeds globally and provides uncertainty estimates to the downscaled data from the various bias-corrected GCMs. Note that, as discussed in the main text, the estimate for this variable is only derived from simulated TCs in areas included in the mask reported in Figure 1 of the main text.

[38] The primary environment predictor used is the maximum potential intensity calculated from monthly vertical profiles of temperature and humidity at each location, including surface temperature.

Annex II: GDP Downscaling Approach

This annex provides more details on the methodology developed by Murakami and others (2021) to construct a forward-looking projection of gridded GDP. One of the key procedures in this endeavor, beyond projecting GDP at the country level in each climate scenario and future period, is to properly account for the geographical pattern of value-added creation, i.e., downscaling country-level GDP to the individual 5 arcminutes cells.

Annex Figure 1, adapted from the authors' paper, shows how the downscaling model is laid out. First, urban population totals in each country are downscaled into cities based on a city growth model. The estimated city populations are then used to estimate urbanization potential that is used to project urban expansion. The city and non-urban populations are further downscaled into 30 arcminutes (0.5 degrees) grids considering projected urban expansion and auxiliary variables (e.g., distance to road/airport/ocean, area of urban/agricultural land, distance and trade among cities). Population data is then combined with GDP. We refer the readers to Murakami and Yamagata (2021) for a more in-depth description of the procedure.

Annex Figure 1: Downscaling model

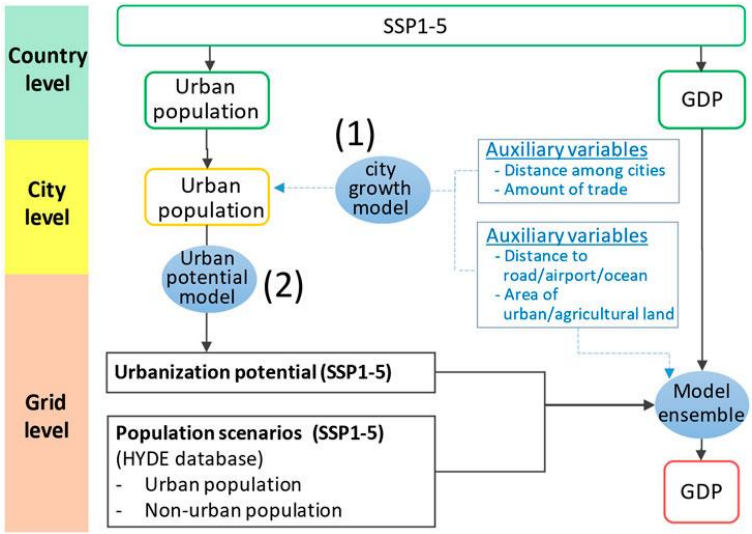

Source: Murakami and others (2021)

Annex III. Drivers of flood results

This annex discusses the key drivers of our flood damages estimates. Country-level damage rates changes over time and scenarios are mainly driven by corresponding changes of the hazard severity (flood depth), as reflected in Annex Figure 2, displaying similar patterns to Figure 9 in the main text. We also consider changes in economic exposures (GDP) which are projected to change over time in line with the Shared Socioeconomic Pathways of each scenario (Murakami, 2021).[39] There also other factors that can have an important impact on damage rates. For floods, based on our data and methodology, these are the fraction flooded in each location in the country and the interplay between river and coastal floods trends (Annex Figure 3).[40]

Annex Figure 2: Floods' depth levels change in meters between baseline and 2050 under SSP2-4.5

Percentage points

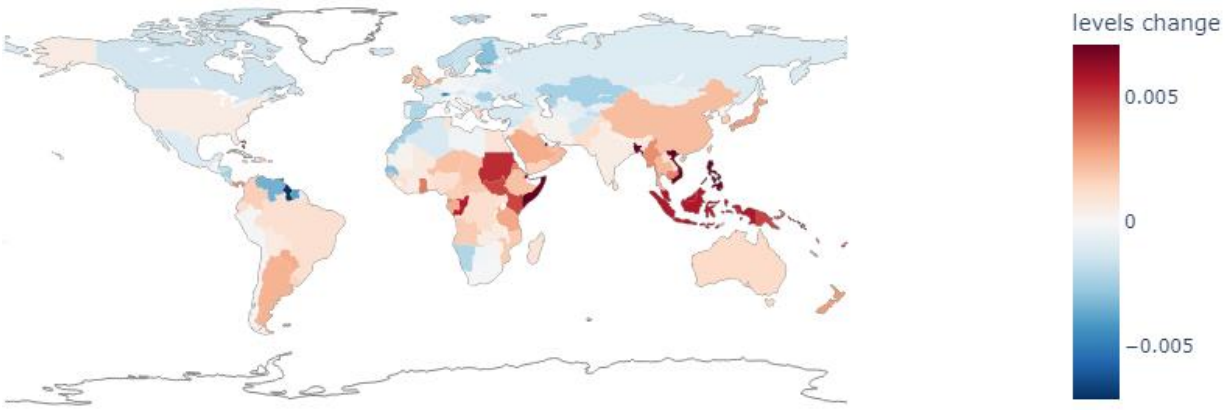

Source: IMF staff

[39] This is different from the methodology used from the NGFS for estimating hazards' damages which keeps GDP fixed as of 2005.
[40] We also note that results at country level may mask regional climate trends and biases from the locations' selection.

Annex Figure 3: Fraction flooded 2020 (LHS) and change between 2020 to 2100 under SSP2-4.5 (RHS) for coastal, river and combined floods

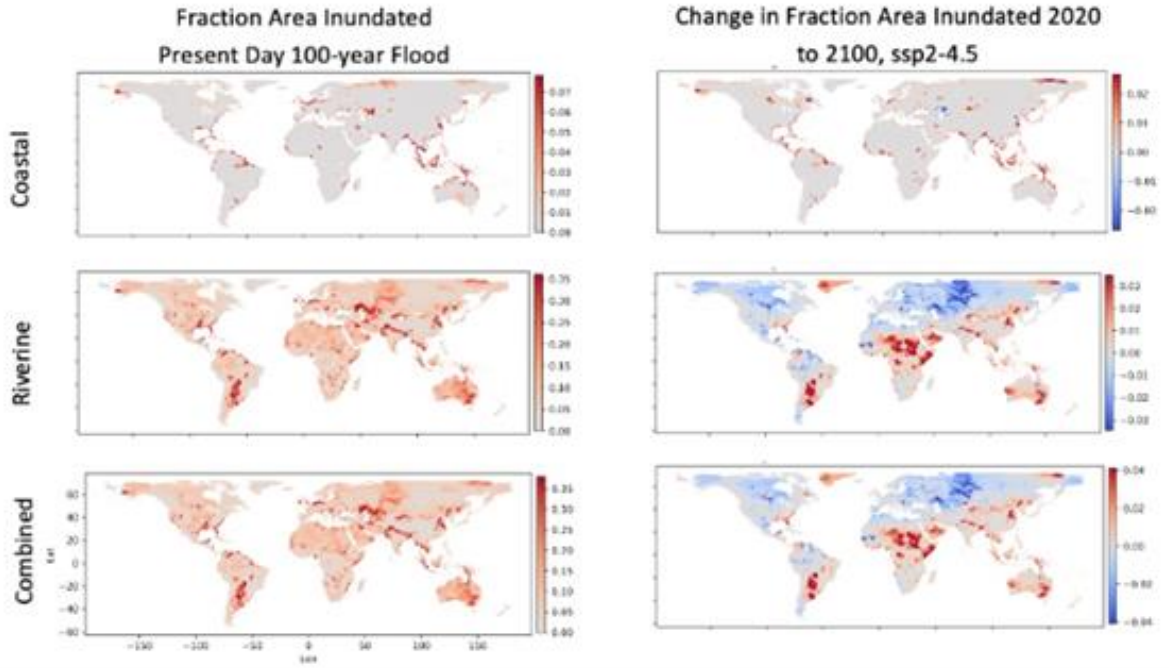

Source: Jupiter Intelligence

Our results show that for most countries damage rates increase over time and as we consider more severe scenarios, pointing to a positive correlation between global flood risks and global warming in line with other global studies (Alfieri and others, 2017; Dottori and others, 2018). An important driver of these observations is the change in (average) flood depth over time, which displays generally increasing trends across time and scenarios. The GDP distribution in these cases does not tend to change these trends. This is the case for example for Bangladesh (Annex Figure 4).

Annex Figure 4: Floods damage rate and hazard severity evolution for Bangladesh

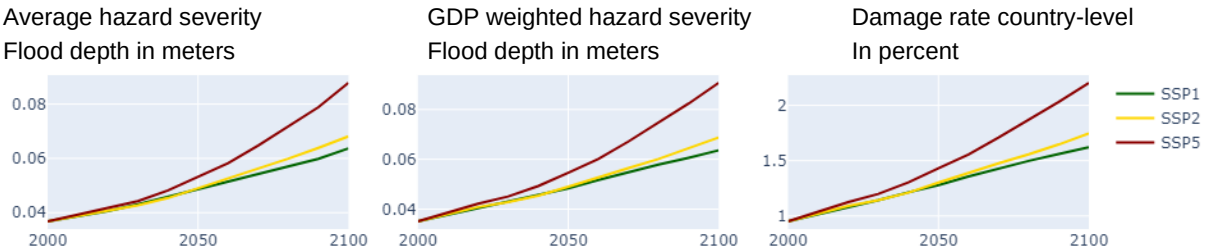

Source: IMF staff

However, there are exceptions. For some countries damages from floods can decrease over time and with more severe scenarios. Certain regions of the world, including in high-latitude regions such as Canada and

some parts of Europe, are expected to experience drier climates which can lead to a decrease in riverine floods risks (Annex Figure 5).

Annex Figure 5: Floods damage rate and hazard severity evolution for Canada

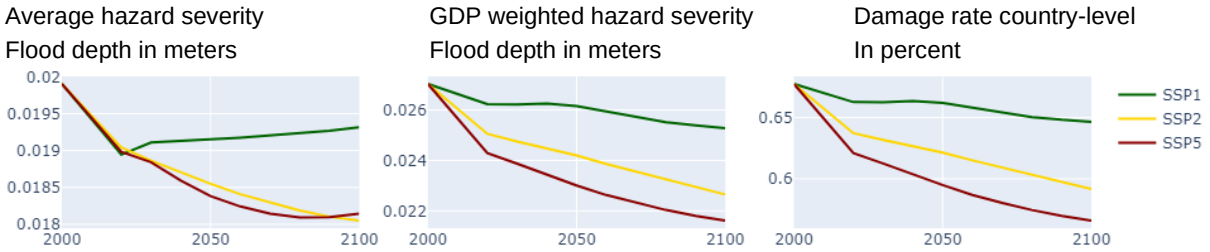

Source: IMF staff

Moreover, the GDP distribution can also alter the damage rates' trends across time and scenarios. For example, for Guatemala, while the average flood depth is increasing across time and scenarios (in 2100), the GDP distribution shifts the damage rates, resulting in lower damages under SSP5-8.5 than under SSP1-2.6. This shows that more extreme SSP scenarios can be associated with higher flood depth but in areas with lower GDP, compared to less severe SSP scenarios (Annex Figure 6).

Annex Figure 6: Floods damage rate and hazard severity evolution for Guatemala

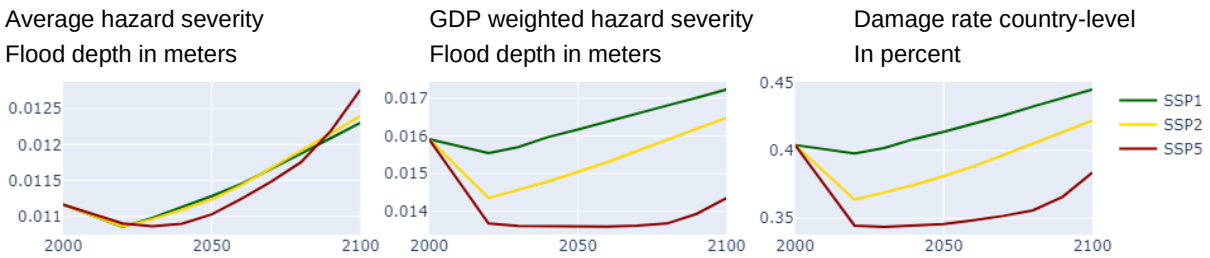

Source: IMF staff

We also observe cases where damages do not display a clear trend across time and scenarios, as for example in Belize. These observations can be driven by the floods data. First, the interplay between river flood and coastal flood trends, which are aggregated in our data, may have different trends. As can be seen in Annex Figure 3 while the fraction flooded from coastal floods tend to increase for all countries by the end of the century, the fraction flooded from river floods displays more heterogeneous changes. For example, at the tropics inland river flood depths can decrease due to decreased precipitation trends. This is the case for Belize for example. Further, coastal water levels, due to sea level rise, tend to increase the most and in a non-linear fashion in the second half of the century (Oppenheimer and others, 2019). Hence, the interplay between coastal and river floods can give rise to non-linear trends over time. Second, while we generally expect flood metrics under different SSPs for a given year (and return period) to be in either increasing or decreasing order, there are cases where this does not hold. While the SSP scenarios relate to increasing levels of CO2 in the atmosphere, the connection to temperature, precipitation, runoff, and flooding from extreme events can be non-linear. Additionally, due to the coarse model resolution of global climate models, the methods needed to

downscale to local streams, and then average multiple climate models, differences in the order of SSPs can occur for individual locations.

Annex Figure 7: Floods damage rate and hazard severity evolution for Belize

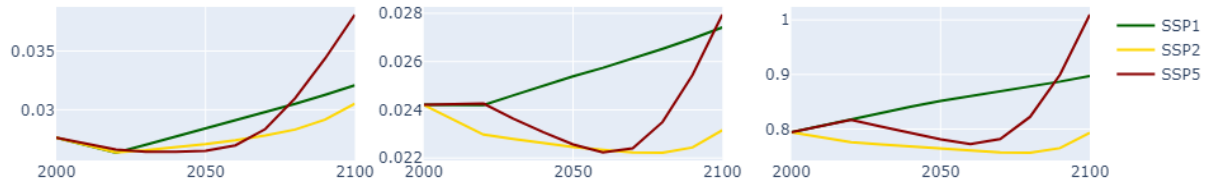

Source: IMF staff

Annex IV. Drivers of TCs results

This annex discusses the key drivers of our TCs damages estimates. Hazard severity (maximum sustained windspeed at 10m above ground) is the major determinant of our results. As it can be gleaned from Annex Figure 8, the countries that will face the highest increase in damage rates are also those for which the hazard metric is projected to increase the most.

Annex Figure 8: Windspeed levels change in 2050, SSP2-4.5

Percentage points

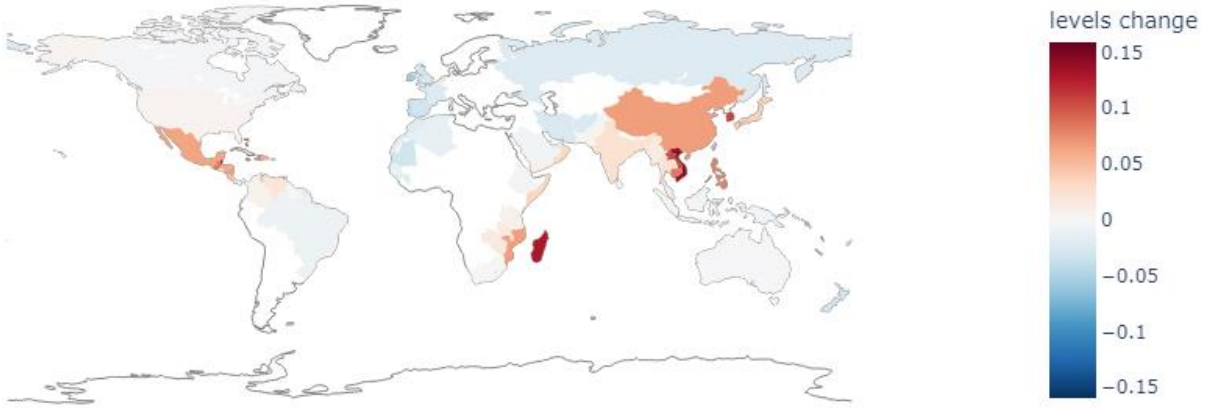

Source: IMF staff

Our results show that for most exposed countries damage rates increase over time and over more severe scenarios, pointing to a positive correlation between global TC risks and global warming. Like the results for floods, an important driver of these observations is the change in (average) maximum windspeed, which displays generally increasing trends across time and scenarios. This is the case for Madagascar, for example, which shows a clear increasing trend for scenarios SSP2-4.5 and SSP5-8.5, with a leveling out expected for SSP1-2.6. Importantly, the shape of these figures is consistent across hazard (left), hazard weighted by the exposure metric (center) and the damage rate (right), as seen in Annex Figure 9 below.

Annex Figure 9: Tropical Cyclones damage rate and hazard severity evolution for Madagascar

Average hazard severity
Wind speed in m/s

GDP weighted hazard severity
Wind speed in m/s

Damage rate country-level
In percent

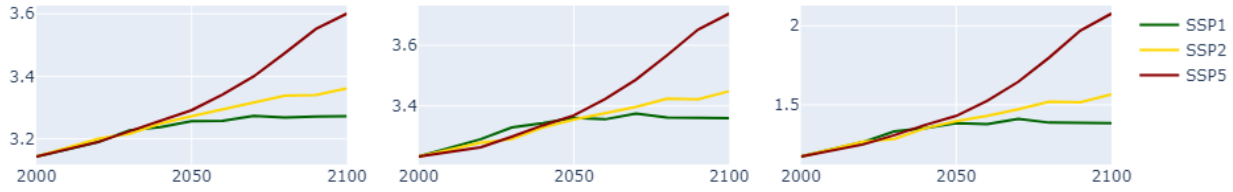

Source: IMF staff

The interplay between the nonlinear damage function, the exposure metric's geographical evolution, and the underlying hazard data sometimes gives rise to more intricate dynamics. Notably for the case of Bangladesh, shown below in Annex Figure 10, we see that the underlying evolution of the hazard points to a decreasing risk between the baseline and 2020, followed by a steady increase towards the end of the century. The interplay with the exposure metric and the damage function changes the differences between scenarios through time, which we can see when comparing the three charts.

Annex Figure 10: Tropical Cyclones damage rate and hazard severity evolution for Bangladesh

Average hazard severity
Wind speed in m/s

GDP weighted hazard severity
Wind speed in m/s

Damage rate country-level
In percent

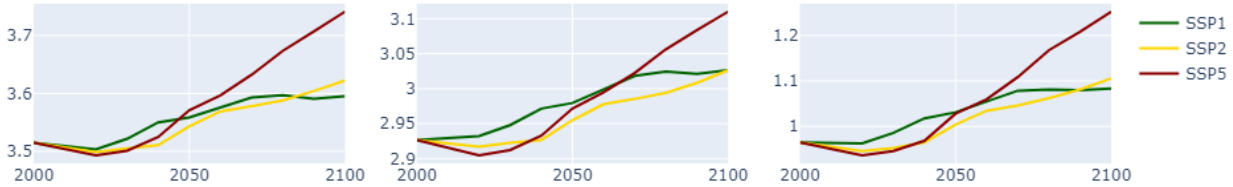

Source: IMF staff

Annex V. Floods' results for SSP1-2.6 and SSP5-8.5

Annex Figure 11: Floods' results for SSP1-2.6 and SSP5-8.5

Damage rate SSP1-2.6
In percent

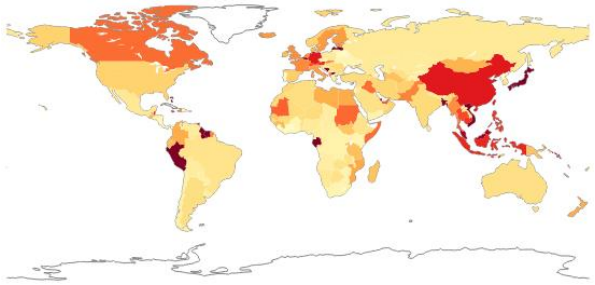

Damage rate SSP5-8.5
In percent

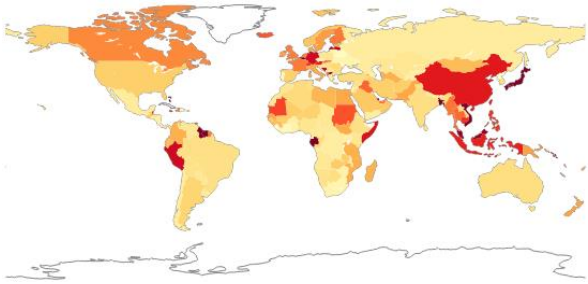

Damage rate relative change SSP1-2.6
In percent

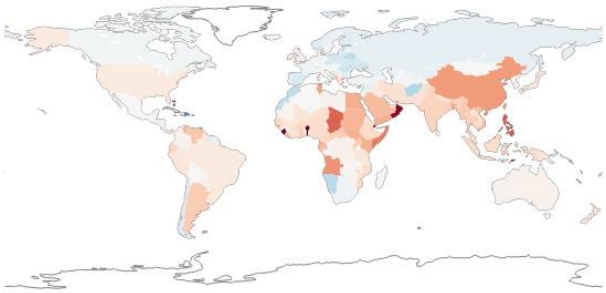

Damage rate relative change SSP5-8.5
In percent

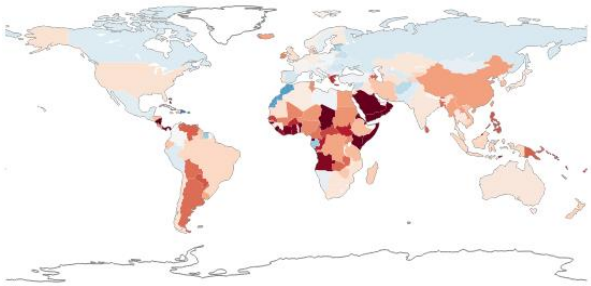

Damage rate levels change SSP1-2.6
Percentage points

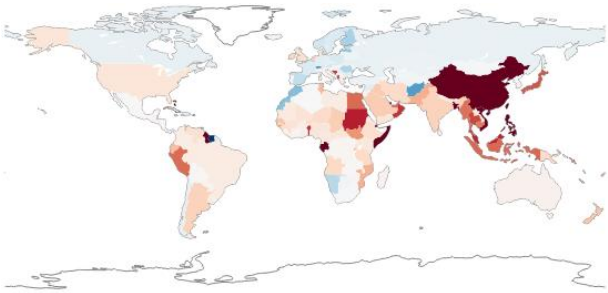

Damage rate levels change SSP5-8.5
Percentage points

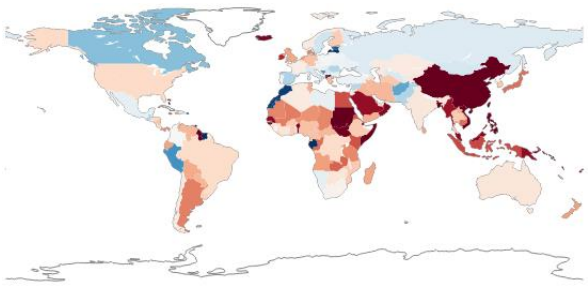

Flood depth levels change SSP1-2.6
In meters

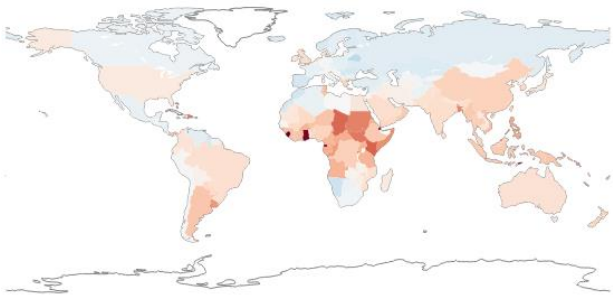

Flood depth levels change SSP5-8.5
In meters

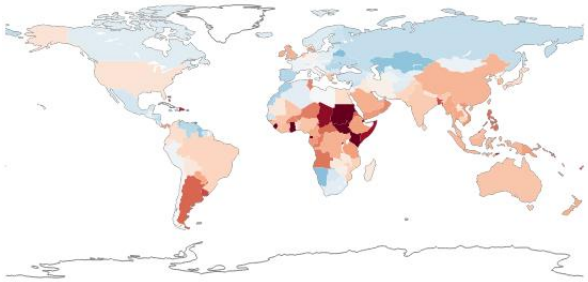

Source: IMF staff

Annex VI. TCs' results for SSP1-2.6 and SSP5-8.5

Annex Figure 11: Tropical cyclones results for SSP1-2.6 and SSP5-8.5

Damage rate SSP1-2.6
In percent

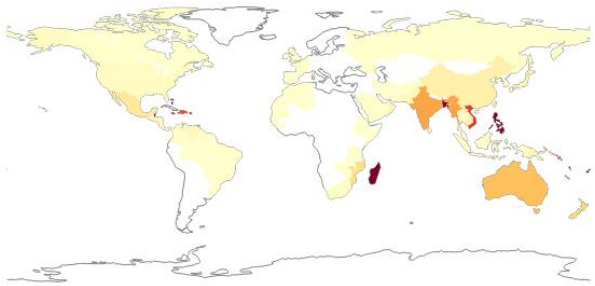

Damage rate SSP5-8.5
In percent

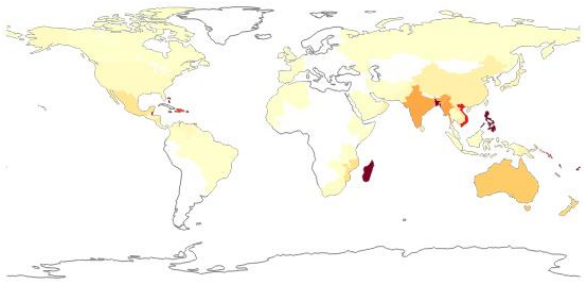

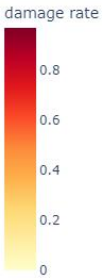

Damage rate relative change SSP1-2.6
In percent

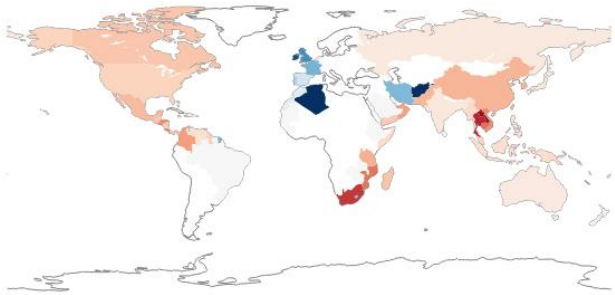

Damage rate relative change SSP5-8.5
In percent

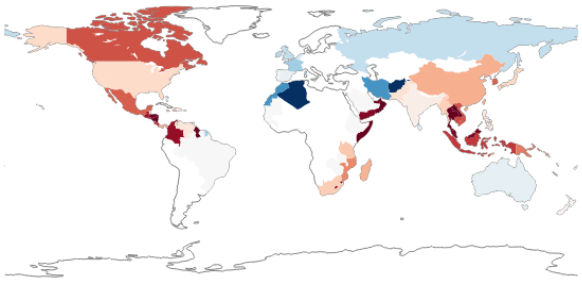

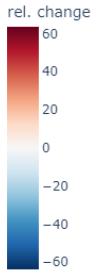

Damage rate levels change SSP1-2.6
Percentage points

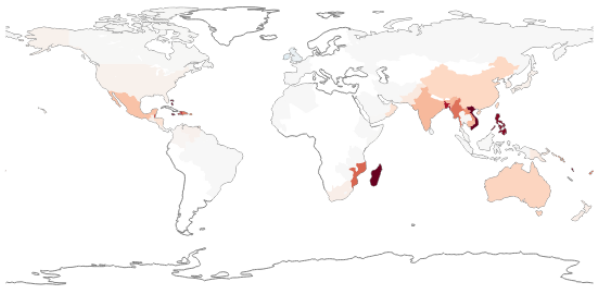

Damage rate levels change SSP5-8.5
Percentage points

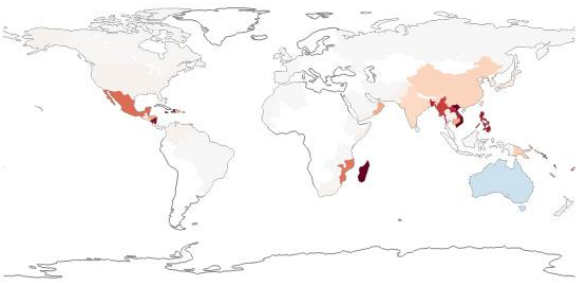

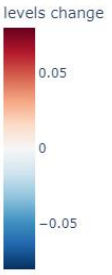

Wind speed levels change SSP1-2.6
In m/s

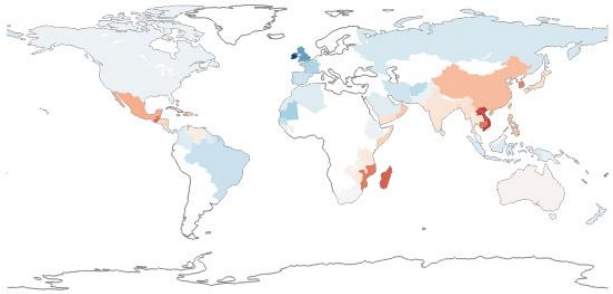

Wind speed levels change SSP5-8.5
In m/s

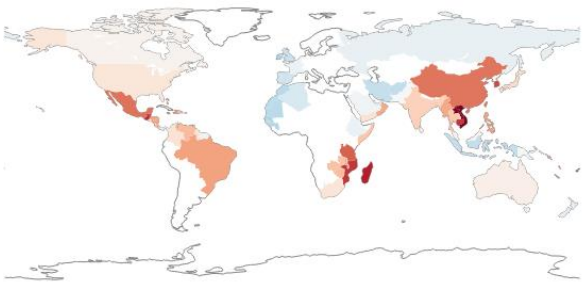

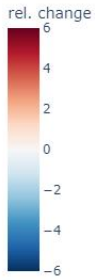

Source: IMF staff

Annex VII: Comparison with the NGFS Results

Estimation of damages from acute physical risks by the NGFS is based on publicly available data from the ISIMIP's, i.e. national GDP estimates downscaled and converted to capital stocks. The 2005 national GDP is downscaled in combination with population distributions data from the History Databased of the Global Environment. GDP data are translated into gridded capital stock using PennWorld Table.[41] Damage projections are calculated assuming that both the size and the repartition of GDP would stay constant as of 2005. This is different from our approach, which accounts for forward-looking projections of GDP under different SSPs.

For TCs, the NGFS generated probabilistic track sets from historical data from IBTrACS. The NGFS adopted the open-source natural catastrophe modelling tool CLIMADA to generate probabilistic TC' track set from historical data. These data are used to compute the wind fields at centroid points defined on the same grid of the exposures data. At each exposure point, the damage is computed from the maximum sustained 1-minute wind speed value at the corresponding centroid point using the same regionally calibrated vulnerability curves adopted in this study (i.e., Eberenz and others, 2021). The damage per country is the aggregated sum over all centroids contained in the country for both the average annual impact and the 1/100 years impact.

For river floods the NGFS use global maps of flooded areas and food depth from multi-model simulations of global hydrological models (GHMs) participating in ISIMIP2b. [42] For each simulation of daily fluvial discharge and each grid cell, a generalized extreme value distribution is fitted to the historical time series of the annual maximum discharge. These are then mapped to the return period of each event to the corresponding flood depth. Finally, empirical data on flood protection is used at the subnational scale (from FLOPROS) through a threshold approach.[43] To quantify damages continent-level residential flood depth damage functions developed by Huizinga and others (2017) are used, as in this paper. [44]

We compared the damage rate relative change from floods and TCs with the relative change in the annual expected damages from river floods and TCs from NGFS.[45] For each year and scenario, we subset to the common countries in both analyses. Then we compute the number of countries where both approaches agree in terms of the relative change sign (both estimates are positive, negative, or zero) or where estimates' signs disagree, for every year and scenario. We define the two analyses consistent when they agree on the sign of relative changes. Last, we computed the median of the relative change for all years and scenarios to evaluate the magnitude of the estimates. It is key to consider that, in addition to differences in the methodological approach for each hazard, there are some general considerations to account for:

[41] For each country the annual ratio of GDP and capital stock was smoothed using a 10-year rolling mean to generate a conversion factor, which was then applied to translate exposed GDP into asset values for 2005. The final dataset is a global distribution of capital stock on a 150 arcsecond resolution in 2005.

[42] The output from the different GHMs is harmonized with respect to their fluvial network using the fluvial routing model CaMa-Flood (version 3.6.2) yielding daily fluvial discharge at 15arcminutes (approx. 25 x 25 km) resolution. For the global annual flood maps, the annual maximum daily discharge for each grid cell is used.

[43] When the protection level is exceeded, the flood occurs as if there were no initial protection, and below the threshold no flooding takes place.

[44] The quantification of flood damages includes the following three steps. First, determine exposed assets on the grid-level based on the flooded fraction obtained from the river flood model. Second, determine the grid level damage by multiplying the exposed assets by the flood fraction and the flood-depth damage function. Finally, aggregate over all grid cells to estimate damages at the country level.

[45] Damages rates and absolute change figures are not readily available through the NGFS.

1. First, the NGFS estimates are available for RCPs but not for SSPs. Hence, the comparison considers matching the SSPs (SSP1-2.6, SSP2-4.5, and SSP5-8.5) with the corresponding RCPs used by NGFS (RCP 2.6, RCP 4.5, and RCP 8.5).
2. Second, the NGFS considers uncertainty in GMT response to a given scenario, and uncertainty in impact projections from all GCMs over GMT levels in each RCP, which gives a range of future damages; in contrast, our estimates come from a single climate parameter computed from a group of GCMs. For the purpose of this comparison, we used the median of the NGFS damages.
3. In addition to using different exposure datasets, exposure data is dynamic in this paper while it is static in NGFS, with fixed exposure in 2005.
4. The baselines for the relative change differ between the analyses; while this paper uses the baseline with the exposure in 2020 and the climate data from a historical window, the NGFS relative changes correspond to 2015.

For floods, the analysis shows that, on average, both estimates agree for 65 percent of the countries (with a maximum of 70 percent and a minimum of 60 percent depending on the year and scenario). There is no clear pattern in the countries where there is divergence in the results. Both approaches show that most of the countries would be negatively impacted by climate change (i.e., an increase in damages with global warming\time?), with an average of 64 percent of the countries from this study (max. of 68 percent and min. of 52 percent) and 60 percent of countries from NGFS estimates (max of 63 percent and min. of 53 percent) considering different years in the estimation horizon and scenarios. For the median relative change, NGFS estimates tends to be higher across years and scenarios with a gap between our estimates and the NGFS's estimates of -5.79 percentage points on average and the smallest for SSP5-8.5 with -3.17 percent. The differences in the methodological approach (e.g., NGFS covering river floods only whereas this study covering river and coastal floods) explain the difference.

TCs results are similar. In most cases, with an average consistency of 55 percent across years and scenarios (a maximum of 57 percent and a minimum of 51 percent), the two analyses find the same sign for relative changes in damages. There is a clear pattern in the countries where results diverge. The NGFS results expect an increasing trend for TC damages in Europe and Northwest Africa and a decreasing trend in Southeast Africa and Oceania, which could be attributable to differences in the underlying synthetic TCs generation methods in the mentioned geographies. For the median relative change, the NGFS estimates tend to be higher across years and scenarios, with the gap between the estimates of 3.34 percentage points.

Table 5: Consistency for floods

Scenario	Year	Obs.	This study + NGFS +	This study - NGFS -	This study + NGFS -	This study - NGFS +	This study 0 NGFS 0	Consistency
SSP1-2.6	2020	173	41.04%	12.72%	9.83%	23.12%	7.51%	61.27%
SSP1-2.6	2030	173	45.66%	8.09%	6.94%	26.01%	7.51%	61.27%
SSP1-2.6	2040	173	48.55%	5.78%	6.94%	25.43%	6.94%	61.27%
SSP1-2.6	2050	173	48.55%	5.78%	6.94%	25.43%	6.36%	60.69%
SSP1-2.6	2060	173	50.29%	6.36%	8.09%	21.97%	6.36%	63.01%
SSP1-2.6	2070	173	52.02%	5.78%	8.67%	20.23%	5.78%	63.58%
SSP1-2.6	2080	173	53.18%	6.36%	8.09%	19.08%	5.78%	65.32%
SSP1-2.6	2090	173	53.18%	5.78%	8.67%	19.08%	5.78%	64.74%
SSP1-2.6	2100	173	53.18%	5.20%	9.25%	19.08%	5.78%	64.16%
SSP2-4.5	2020	171	45.61%	7.60%	14.62%	19.30%	7.02%	60.23%
SSP2-4.5	2030	171	50.88%	4.68%	10.53%	21.05%	7.02%	62.57%
SSP2-4.5	2040	171	53.80%	6.43%	8.19%	18.71%	6.43%	66.67%
SSP2-4.5	2050	171	53.22%	8.77%	7.60%	17.54%	5.85%	67.84%
SSP2-4.5	2060	171	53.80%	6.43%	7.60%	19.30%	5.26%	65.50%
SSP2-4.5	2070	171	52.63%	5.26%	8.19%	21.05%	5.26%	63.16%
SSP2-4.5	2080	171	52.63%	7.60%	8.19%	18.71%	5.26%	65.50%
SSP2-4.5	2090	171	52.63%	8.77%	8.19%	17.54%	5.26%	66.67%
SSP2-4.5	2100	171	52.63%	8.77%	8.19%	17.54%	5.26%	66.67%
SSP5-8.5	2020	168	48.21%	5.95%	16.67%	16.67%	7.14%	61.31%
SSP5-8.5	2030	168	54.76%	5.36%	8.93%	18.45%	6.55%	66.67%
SSP5-8.5	2040	168	55.95%	8.33%	7.74%	15.48%	5.95%	70.24%
SSP5-8.5	2050	168	55.95%	4.76%	8.33%	18.45%	5.36%	66.07%
SSP5-8.5	2060	168	53.57%	7.14%	11.31%	15.48%	4.76%	65.48%
SSP5-8.5	2070	168	52.98%	9.52%	12.50%	12.50%	5.36%	67.86%
SSP5-8.5	2080	168	54.17%	10.12%	10.71%	12.50%	5.36%	69.64%
SSP5-8.5	2090	168	52.98%	8.33%	11.31%	14.88%	5.36%	66.67%
SSP5-8.5	2100	168	49.40%	9.52%	15.48%	13.10%	5.36%	64.29%

Notes: The number of observations changes given that we subset to common countries in this study and NGFS. The sign + and – mean that the sign of the relative changes in damage rates is positive and negative respectively.

Table 6: Consistency for TCs

Scenario	Year	Obs.	This study + NGFS +	This study - NGFS -	This study + NGFS -	This study - NGFS +	This study 0 NGFS 0	Consistency
SSP1-2.6	2020	77	50.65%	1.30%	20.78%	19.48%	1.30%	53.25%
SSP1-2.6	2030	77	53.25%	1.30%	20.78%	16.88%	1.30%	55.84%
SSP1-2.6	2040	77	54.55%	1.30%	20.78%	15.58%	1.30%	57.14%
SSP1-2.6	2050	77	54.55%	1.30%	20.78%	15.58%	1.30%	57.14%
SSP1-2.6	2060	77	55.84%	1.30%	20.78%	14.29%	0.00%	57.14%
SSP1-2.6	2070	77	53.25%	1.30%	20.78%	16.88%	0.00%	54.55%
SSP1-2.6	2080	77	51.95%	0.00%	22.08%	18.18%	0.00%	51.95%
SSP1-2.6	2090	77	51.95%	1.30%	20.78%	18.18%	0.00%	53.25%
SSP1-2.6	2100	77	51.95%	1.30%	20.78%	18.18%	0.00%	53.25%
SSP2-4.5	2020	77	46.75%	2.60%	19.48%	23.38%	1.30%	50.65%
SSP2-4.5	2030	77	50.65%	1.30%	20.78%	19.48%	1.30%	53.25%
SSP2-4.5	2040	77	54.55%	1.30%	20.78%	15.58%	0.00%	55.84%
SSP2-4.5	2050	77	55.84%	1.30%	20.78%	14.29%	0.00%	57.14%
SSP2-4.5	2060	77	54.55%	1.30%	20.78%	15.58%	0.00%	55.84%
SSP2-4.5	2070	77	55.84%	1.30%	20.78%	14.29%	0.00%	57.14%
SSP2-4.5	2080	77	57.14%	1.30%	20.78%	12.99%	0.00%	58.44%
SSP2-4.5	2090	77	55.84%	1.30%	20.78%	14.29%	0.00%	57.14%
SSP2-4.5	2100	77	54.55%	1.30%	20.78%	15.58%	0.00%	55.84%
SSP5-8.5	2020	77	44.16%	5.19%	16.88%	25.97%	1.30%	50.65%
SSP5-8.5	2030	77	49.35%	3.90%	18.18%	20.78%	1.30%	54.55%
SSP5-8.5	2040	77	53.25%	1.30%	20.78%	16.88%	0.00%	54.55%
SSP5-8.5	2050	77	53.25%	1.30%	20.78%	16.88%	0.00%	54.55%
SSP5-8.5	2060	77	54.55%	1.30%	20.78%	15.58%	0.00%	55.84%

Notes: The number of observations changes given that we subset to common countries in this study and NGFS. From 2060 for SSP5-8.5, the NGFS does not have estimates for TCs, so there is no comparison for years beyond 2060 for this scenario. The sign + and – mean that the sign of the relative changes in damage rates is positive and negative respectively.

Annex VIII. Limitations

This Annex discusses limitations and caveats of the analysis that are important for the interpretation of the results, as well as possible ways to address them in future analysis.

First, there are limitations and uncertainties related to the hazards' data. It is important to acknowledge that there is a very wide range of climate models to choose from giving rise to sizable model uncertainty. To account for this, Jupiter Intelligence adopts data from different GCMs from CMIP6 and CMIP5 forcings. To select specific models, Jupiter Intelligence considers the availability of predictors, scenarios, and data; ensemble members, and model quality. Further, Jupiter Intelligence provides uncertainty bounds. These bounds consider different types of uncertainty depending on the hazard: hydrological model parameter uncertainty for flood depth and Generalized Extreme Value (GEV) fitting uncertainty for the wind. Future extensions of this study could take these uncertainty bounds into account.

In addition, the spatial resolution and geographical coverage of the hazards' data impact the results. Floods tend to have a very localized nature and fully estimating their impact calls for using highly granular geospatial data. In this study we adopt granular data with a spatial resolution of 3 arcseconds (90 meters by 90 meters at the equatorial sea level). However, availability of 100,000 locations globally, implies that the geographical coverage is not always ideal. Having additional locations would improve the analysis.[46] By contrast, for TCs there is no such concern as the spatial resolution of the hazard data used by Jupiter Intelligence is 15 arcminutes before bilinear interpolation. Therefore, the effective coverage for TCs is much higher than for floods because the risk cannot change within a single GDP cell.

Estimating damages relies on some assumptions on hazards data. For example, the lowest return period available for the data provided by Jupiter Intelligence is 1-in-10 years, and the expected damage rate for return periods below 1-in-10 years is set to zero. This consideration implies an underestimation of the damages, when low-severity events cause recurrent losses. Further, correlation of the hazard data across locations is assumed to be zero, which implies an overestimation of the damages. The overall effect of these assumptions on damages is unclear. Having hazards data for additional return periods as well as information on spatial correlation would improve the analysis.

Aggregating the impact of various hazards is challenging. Most climate studies in the literature have focused on single hazards, however there is a rapidly growing policy and scientific recognition on the need to consider multi-hazard and their potential cascading effects (Wald and others (2020)). With regards to floods, for instance, there has recently been more focus on compound floods, whereby the interaction of coastal, river, and pluvial floods can influence the overall hazard and risk (Zscheischler and others, 2018). Jupiter Intelligence data tackle this issue by taking the maximum value across different severities. Specifically, they provide the maximum depth of inundation between river and coastal floods, which account for both sea level rise, storms and tide. This approach for combining fluvial and coastal results evaluates the two hazards independently and is thus a reasonable estimate of flood risk if the two are not covariate. However, in places where fluvial and coastal flooding can be coincident, the joint hazard distribution becomes important, and the present methods may underestimate the true risk from flooding. Furthermore, for some locations it can be important to jointly

[46] We note that the locations, in line with the aim of in this study, were selected to maximize coverage of economic activity, where a gridded GDP coverage above 95 percent is achieved with 100K locations. We do not expect a significant bias in the results due to selection of locations to maximize coverage of economic activity.

consider both floods and winds damages. Floods and TCs damages are calculated in isolation in this study. Caution should be applied if interested in combining damages from both floods and TCs together.

Second, the exposures used in this study is only a proxy for real economic exposures. The downscaled GDP data has the benefit of being forward-looking and scenario dependent, as well as available globally. However, when available for specific countries, using granular geospatial data on buildings, infrastructures and other relevant economic exposures would be ideal.

Third, the damage functions that are used capture exposures' vulnerabilities are simplified expression of economic damages as a function of climate inputs. However, use of regionally calibrated damage functions brings some limitations. For example, TC damage functions adopted from Eberenz and others (2021) are calibrated using reported damages from EM-DAT data. Hence, limitations of the EM-DAT data such as biases and under-reporting for some countries extend to the associated damage functions. As noted in Eberenz and others (2021) the damage functions show considerable differences in the level of uncertainty across model regions, with the largest uncertainties for the North-West Pacific regions. It is also important to keep in mind that the damage functions used in this study focus on estimating direct damages and excludes indirect damages, for example, damages from business interruption. Accounting for these indirect channels would lead to an increase in damages and it is left for future research.

Finally, this study does not explicitly account for adaptation and mitigation measures.[47] Excluding future adaptation and mitigation measures, and the associated uncertainties, provide an upper-bound estimate of damages which can hence be used to illustrate the benefits of these measures. When focusing on specific countries, where data and plans on these measures are available, the methodology could be extended to incorporate them.

[47] Only for floods in the USA, England, the Netherlands and Germany our hazard data accounts for the assumption that locations currently protected by levees will be protected up to and including a 100-year flood in the future.

References

Adrian, T., Grippa, P., Gross, M., Haksar, V., Krznar, I., Lepore, C., Lipinsky, F., Oura, H., Lamichhane, S., and Panagiotopoulos, A. 2022. Approaches to Climate Risk Analysis in FSAPs. Staff Climate Notes. International Monetary Fund.

Alfieri, L., Bisselink, B., Dottori, F., Naumann, G., de Roo, A., Salamon, P., Wyser, K., and Feyen, L. 2017. Global projections of river flood risk in a warmer world. Earth's Future 5(2), 171–182.

Aligishiev, Z., Ruane, C., and Sultanov, A. 2023. "User Manual for the DIGNAD Toolkit." IMF Technical Notes and Manuals 2023/03, International Monetary Fund, Washington, DC.

Arias, P.A., Bellouin, N., Coppola, E., Jones, R., Krinner, G., Marotzke, J., Naik, V., Palmer, M.D., Plattner, G.-K., Rogelj, J., Rojas, M., Sillmann, J., Storelvmo, T., Thorne, P.W., Trewin, B., Achuta Rao, K., Adhikary, B., Allan, R.P., Armour, K.,…,and Zickfeld, K. 2021. Technical summary. In Climate Change 2021: The Physical Science Basis. Contribution of Working Group14 I to the Sixth Assessment Report of the Intergovernmental Panel on Climate Change. Cambridge University Press, Cambridge, United Kingdom and New York, NY, USA,33-144.

Bachner, G., Knittel, N., Poledna, S., Hochrainer-Stigler, S., and Reiter, K. 2023. Revealing indirect risks in complex socioeconomic systems: A highly detailed multi-model analysis of flood events in Austria. Risk Analysis.

Bakkensen, L.A., and Mendelsohn, R.O. 2019. Global tropical cyclones damages and fatalities under climate change: An update assessment. Hurricane risk, 179-197.

BIS. 2021. Climate-related financial risks – measurement methodologies. Bank for International Settlements.

Buchhorn, M., Smets, B., Bertels, L., De Roo, B., Lesiv, M., Tsendbazar, N.-E., Herold, M., and Fritz, S. 2020. Copernicus global land service: Land cover 100m: collection 3: epoch 2019: Globe. Version V3 01 Data Set.

Burke, M., Hsiang, S.M., and Miguel, E. 2015. Global non-linear effect of temperature on economic production. Nature 527, 235–239. https://doi.org/10.1038/nature15725

Cammalleri, C, Naumann, G., Mentaschi, L., Formetta, G., Forzieri, G., Gosling, S., Bisselink, B., De Roo, A., and Feyen, L. 2020. Global Warming and Drought Impacts in the EU. Publications Office of the European Union: Luxembourg.

Czajkowski, J., Done, J., 2014. As the Wind Blows? Understanding Hurricane Damages at the Local Level through a Case Study Analysis. Weather Clim. Soc. 6, 202–217. https://doi.org/10.1175/WCAS-D-13-00024.1

Ding, Y., Hayes, M., and Widhalm, M. 2011. Measuring Economic Impacts of Drought: A Review and Discussion. Disaster Prevention and Management: An International Journal 20(4), 434-446.

Dottori, F., Szewczyk, W., Ciscar, J.-C., Zhao, F., Alfieri, L., Hirabayashi, Y., Bianchi, A., Mongelli, I., Frieler, K., Betts, R.A., and Feyen, L. 2018. Increased human and economic losses from river flooding with anthropogenic warming. Nature Climate Change 8(9), 781–786. https://doi.org/10.1038/s41558-018-0257-z

Duenwald, Mr Christoph, et al. Feeling the Heat: Adapting to Climate Change in the Middle East and Central Asia. International Monetary Fund, 2022.

Eberenz, S., Lüthi, S., and Bresch, D.N. 2021. Regional tropical cyclone impact functions for globally consistent risk assessments. Natural Hazards and Earth Systems Sciences 21(1), 393–415.

Emanuel, K. 2011. Global warming effects on US hurricane damage. Weather, Climate, and Society 3(4), 261–268.

FEMA. 2011. Multi-hazard Loss Estimation Methodology Hurricane Model Hazus®–MH 2.1 User Manual. Department of Homeland Security, Federal Emergency Management Agency, Mitigation Division, Washington, DC.

Gettelman, A., Bresch, D.N., Chen, C.C., Truesdale, J.E., and Bacmeister. J.T. 2017. Projections of Future Tropical Cyclone Damage with a High-Resolution Global Climate Model. Climatic Change, 146, 575-585.

Hallegatte, S. 2007. The Use of Synthetic Hurricane Tracks in Risk Analysis and Climate Change Damage Assessment. Journal of Applied Meteorology and climatology, 46(11), 1956–1966.

Hallegatte, S., Lipinsky, F., Morales, P., Oura, H., Ranger, N., Gert Jan Regelink, M., and Reinders, H.J. 2022. Bank Stress Testing of Physical Risks under Climate Change Macro Scenarios: Typhoon Risks to the Philippines. International Monetary Fund.

Howard, P. 2014. Flammable Planet: Wildfires and the Social Cost of Carbon. New York: NYU Law School Institute for Policy Integrity.

Huizinga, J., de Moel, H., and Szewczyk, W. 2017. Global flood depth-damage functions: Methodology and the database with guidelines. Joint Research Centre (European Commission), Sevilla, Spain.

IMF. 2022. Mexico: Financial Sector Assessment Program-Technical Note on Climate Risk Analysis. Country. Report. No 22/360.

IPCC. 2023. Summary for Policymakers. In: Climate Change 2023: Synthesis Report. Contribution of Working Groups I, II and III to the Sixth Assessment Report of the Intergovernmental Panel on Climate Change.

Jones, R.L., Guha-Sapir, D., and Tubeuf, S. 2022. Human and economic impacts of natural disasters: can we trust the global data? Scientific data 9(1), 572.

Kahn, M.E., Mohaddes, K., Ng, R.N.C., Pesaran, M.H., Raissi, M., and Yang, J.-C. 2021. Long-term macroeconomic effects of climate change: A cross-country analysis. Energy Economics 104, 105624.

Kalkuhl, M., and Wenz, L. 2020. The impact of climate conditions on economic production. Evidence from a global panel of regions. Journal of Environmental Economics and Management. 103, 102360.

Lange, S., Volkholz, J., Geiger, T., Zhao, F. Vega, I., Veldkamp, T., and Reyer, C. 2020. Projecting Exposure to Extreme Climate Impact Events Across Six Event Categories and Three Spatial Scales. Earth's Future 8(12): e2020EF001616.

Lüthi, S., Aznar-Siguan, G., Fairless, C., and Bresch, D. N. 2021. Globally Consistent Assessment of Economic Impacts of Wildfires in CLIMADA v2.2. Geoscientific Model Development 14(11), 7175–87.

Marto, R., Papageorgiou, C., and Klyuev, V. 2018. Building resilience to natural disasters: An application to small developing states. Journal of Development Economics 135, 574–586.

Melina, M.G., and Santoro, M. 2021. Enhancing Resilience to Climate Change in the Maldives. International Monetary Fund.

Mendelsohn, R., Emanuel, K., Chonabayashi, S., Bakkensen, L., 2012. The impact of climate change on global tropical cyclone damage. Nat. Clim. Change 2, 205–209. https://doi.org/10.1038/nclimate1357

Murakami, D., Yoshida, T., and Yamagata, Y. 2021. Gridded GDP projections compatible with the five SSPS (Shared Socioeconomic Pathways). Frontiers in Built Environment, 7, 760306.

Nardi, F., Annis, A., Di Baldassarre, G., Vivoni, E., and Grimaldi, S. 2019. GFPLAIN250m, a global high-resolution dataset of Earth's floodplains. Scientific data 6(1), 1–6.

Nardi, F., Vivoni, E.R., and Grimaldi, S. 2006. Investigating a floodplain scaling relation using a hydrogeomorphic delineation method. Water Resources Research, 42(9).

Oppenheimer, M., Glavovic, B., Hinkel, J., Van de Wal, R., Magnan, A.K., Abd-Elgawad, A., Cai, R., Cifuentes-Jara, M., Deconto, R.M., and Ghosh, T. 2019. Sea level rise and implications for low lying islands, coasts and communities. Advances in Climate Change Research 16(2), 163.

Pielke Jr, Roger A. "Future economic damage from tropical cyclones: sensitivities to societal and climate changes." Philosophical Transactions of the Royal Society A: Mathematical, Physical and Engineering Sciences 365.1860 (2007): 2717-2729.

Smith, A., Bates, P.D., and Wing, O. 2019. New estimates of flood exposure in developing countries using high-resolution population data. Nature Communications 10(1), 1814.

Thomas, D., Butry, D., Gilbert, S., Webb, D., and Fung, J. 2017. The Costs and Losses of Wildfires. National Institute of Standards and Technology Special Publication 1215(11).

United Nations Office for Disaster Risk Reduction (UNDRR). 2013. Global Assesment Report on Disaster Risk Reduction 2013. From Shared Risk to Shared Value: the Business Case for Disaster Risk Reduction. United Nations (1901).

United Nations Office for Disaster Risk Reduction (UNDRR). 2022. Global Assesment Report on Disaster Risk Reduction 2022: Our World at Risk: Transforming Governance for a Resilient Future. United Nations (1901).

Ward, P.J., Blauhut, V., Bloemendaal, N., Daniell, J.E., Ruiter, M.C. de, Duncan, M.J., Emberson, R., Jenkins, S.F., Kirschbaum, D., and Kunz, M. 2020. Natural hazard risk assessments at the global scale. Natural Hazards and Earth Systems Sciences 20(4), 1069–1096.

Yamin, L.E., Hurtado, A.I., Barbat, A.H., and Cardona, O.D. 2014. Seismic and wind vulnerability assessment for the GAR-13 global risk assessment. International Journal of disaster risk reduction 10, 452–460.

PUBLICATIONS